UNIVERSITY OF LEEDS

This is a repository copy of *Methane Production from the Pyrolysis–Catalytic Hydrogenation of Waste Biomass: Influence of Process Conditions and Catalyst Type*.

White Rose Research Online URL for this paper:
http://eprints.whiterose.ac.uk/150485/

Version: Accepted Version

Article:
Jaffar, MM, Nahil, MA and Williams, PT orcid.org/0000-0003-0401-9326 (2019) Methane Production from the Pyrolysis–Catalytic Hydrogenation of Waste Biomass: Influence of Process Conditions and Catalyst Type. Energy and Fuels, 33 (8). pp. 7443-7457. ISSN 0887-0624

https://doi.org/10.1021/acs.energyfuels.9b01524

© 2019 American Chemical Society. This is an author produced version of an article published in Energy and Fuels. Uploaded in accordance with the publisher's self-archiving policy.

Reuse
Items deposited in White Rose Research Online are protected by copyright, with all rights reserved unless indicated otherwise. They may be downloaded and/or printed for private study, or other acts as permitted by national copyright laws. The publisher or other rights holders may allow further reproduction and re-use of the full text version. This is indicated by the licence information on the White Rose Research Online record for the item.

Takedown
If you consider content in White Rose Research Online to be in breach of UK law, please notify us by emailing eprints@whiterose.ac.uk including the URL of the record and the reason for the withdrawal request.

White Rose university consortium
Universities of Leeds, Sheffield & York

eprints@whiterose.ac.uk
https://eprints.whiterose.ac.uk/

Methane production from the pyrolysis-catalytic hydrogenation of waste biomass: Influence of process conditions and catalyst type

Mohammad M. Jaffar, Mohamad A. Nahil, Paul T. Williams*

School of Chemical & Process Engineering, University of Leeds, Leeds, LS2 9JT, U.K.

(*Corresponding author; Email; p.t.williams@leeds.ac.uk; Tel; #44 1133432504)

ABSTRACT: The production of methane through the optimization of various operating parameters and the use of different catalysts has been investigated using a two-stage, pyrolysis-catalytic hydrogenation reactor. Pyrolysis of the biomass in the 1st stage produces a suite of gases, including CO_2 and CO, which undergo catalytic hydrogenation in the presence of added H_2 in the 2nd stage. The influence of the biomass pyrolysis temperature, catalyst temperature and H_2 gas space velocity have been investigated for the optimization and enhancement of the methane yield. In addition, different metal catalysts (Co/Al_2O_3, Mo/Al_2O_3, Ni/Al_2O_3, Fe/Al_2O_3), the influence of different metal loadings, catalyst calcination temperature and different support materials (Al_2O_3, SiO_2 and MCM-41) were investigated. The yield of methane was linked to the properties of the catalysts including the preparation calcination temperature and support material which influenced the catalyst surface area and metal crystallite particle size by sintering. The highest methane yield of 7.4 mmol $g^{-1}_{biomass}$ was obtained at a final pyrolysis temperature of 800 °C, catalyst temperature of 500 °C and H_2 gas hourly space velocity of 3600 ml h^{-1} $g^{-1}_{catayst}$. This optimization process resulted in 75.5 vol.% of methane in the output gaseous mixture.

Key words: Biomass; Methanation; Catalyst; Hydrogenation; Methane

1. INTRODUCTION

The increased awareness regarding the depletion of fossil fuels and the problems associated with global warming are the key factors for the promotion of fuels that are sustainable.[1] In the current energy mix, biomass is considered to be a sustainable, renewable and carbon neutral fuel.[2] Biomass fuels also have an advantage over conventional fossil fuels since the biomass feedstock supply can be readily replenished.[3] Biomass may be thermally processed through combustion, pyrolysis and gasification. Pyrolysis is the thermal; degradation of the biomass in the absence of oxygen to produce either solid, liquid and gaseous fuels depending upon the operating parameters and reactor configuration.[4] Gasification is the process of converting the biomass feedstock into gaseous fuel in the presence of a limited supply of oxygen in the form of air, steam or pure oxygen. For example, steam gasification is a process for conversion of biomass at high temperature that results in synthesis gas production mainly including H_2, CO and CO_2.[5]

Whilst there has been much research into the production of hydrogen from biomass,[6,7] there is less research reported into the production of methane from biomass as a substitute for natural gas. Production of substitute natural gas from biomass is an attractive process option because of the already well developed and organized infrastructure and distribution facilities for natural gas.[8,9] The further advantage being that the substitute natural gas would be derived from a sustainable biomass feedstock rather than fossil fuel natural gas.

The catalytic hydrogenation (methanation) of CO and CO_2, has been developed, mainly for the production of methane from coal as the source of the carbon oxides.[10,11] Studies on the optimisation of the methane yield have shown, for example, that catalyst temperatures for the catalytic hydrogenation reaction are in the range of 200 – 500 °C.[12,13] A wide range of hydrogenation catalysts have been investigated, for example, Ni, Fe, and Rh [14-16] and different catalyst support materials, such as Al_2O_3, SiO_2, ZrO_2, CeO_2, and TiO_2.[14] Among the different catalysts Ni, Ru, and Rh are considered as the most effective for methanation. But, Ni based catalyst are much cheaper as compared to that of Ru and Rh based catalysts. Likewise, a suitable support is required to maintain the stability of the metals on the support otherwise non-uniform metal distribution and sintering may occur. According to He et al.,[17] uniform distribution of metal and its strong interaction with a support results in the formation of strong basic sites which results in the enhanced catalytic methanation reaction.

The pyrolysis of biomass produces a gas product consisting of mainly carbon dioxide, carbon monoxide, hydrogen, methane and other hydrocarbons. The production of methane via the catalytic hydrogenation of the product biomass pyrolysis gases, CO and CO_2, coupled with the introduction of H_2 has the potential to generate CH_4 from the catalytic hydrogenation of biomass pyrolysis gases. Therefore, there is interest and novelty in developing a two-stage process, with 1st stage pyrolysis of biomass stage to produce a wide range of hydrocarbon and oxygenated hydrocarbon vapours and gases including CO, CO_2 which are then passed directly to a 2nd stage where catalytic hydrogenation takes place in the presence of introduced hydrogen.

The two-stage pyrolysis-catalytic hydrogenation process will involve a wide range of reactions (Table 1). The pyrolysis of biomass (equation 1) thermally degrades the biomass components, consisting of mainly cellulose, hemicellulose and lignin to produce degradation products including gases, mainly oxygenated hydrocarbons but also some non-oxygenated hydrocarbon polymeric fragments and char. The pyrolysis degradation gases, oxygenated hydrocarbons and non-hydrocarbons enter the catalytic reactor, where many further reactions will occur. For example, the oxygenated hydrocarbons and non-oxygenated hydrocarbons will undergo thermal cracking in the hot zone of the catalytic reactor (e.g. equation 2). The moisture in the biomass will generate steam and along with the reaction products of the biomass thermal degradation will result in steam reforming of the oxygenated hydrocarbons (bio-oil, equation 3) and non-oxygenated hydrocarbons (equation 4), resulting in production of carbon monoxide and hydrogen. Since there are significant quantities of carbon dioxide generated from the biomass pyrolysis process, dry (CO_2) reforming of the oxygenated (bio-oil) and non-oxygenated hydrocarbons may occur (equations, 5 and 6), resulting in further production of carbon monoxide and hydrogen. The reforming reactions will be enhanced in the presence of the catalyst in the 2nd stage reactor. There is also the potential for the water gas shift reaction to produce hydrogen and carbon dioxide (equation 7). The production of carbon monoxide and carbon dioxide from biomass degradation and as reaction products then undergoes methanation reactions through addition of the hydrogen gas to the reactor, resulting in hydrogenation of the carbon oxides in the presence of the catalyst (equations 8 and 9), resulting in methane production. At higher temperatures, there is also the potential for the endothermic Boudouard reaction (equation 10) and for carbon hydrogenation to occur (equation 11).

To our best knowledge no work has been reported for the production of methane from biomass via a two staged pyrolysis-catalytic hydrogenation process. In this paper, we report on the optimisation of a two-stage, biomass pyrolysis-catalytic hydrogenation reactor system for

the production of methane. The effect of various operating parameters including pyrolysis temperature, hydrogenation catalyst temperature, hydrogen gas space velocity, biomass:catalyst ratio were investigated. In addition, the influence of different catalyst metals, different catalyst support materials and different catalyst preparation calcination temperatures in relation to methane yield were studied.

2. MATERIALS AND METHODS

2.1. Biomass sample. The biomass was compressed waste wood sawdust in the form of wood pellets obtained from Liverpool Wood Pellets Ltd, Liverpool, UK. The pellets were milled and sieved to produce a homogenized biomass sample of particle size range between 0.3-0.5mm. The proximate analysis of the biomass was determined by thermogravimetric analysis using a Shimadzu TGA-50 analyser and the results showed, 7.8 wt.% moisture, 0.3 wt.% ash, 93.3 wt.% volatiles and 6.7 wt.% fixed carbon. The elemental analysis of the biomass was obtained with a Vario Micro Elemental Analyzer, and the results showed, 50.1 wt.% carbon, 5.4 wt.% hydrogen, 48.6 wt.% oxygen and 0.1 wt.% nitrogen.

2.2. Catalyst Preparation. The catalyst used for investigating the effect of operating parameters on the catalytic hydrogasification of the biomass pyrolysis gases was 10 wt.% Co/Al_2O_3 prepared by wet impregnation method. A cobalt catalyst was chosen as it has been shown to be effective for the hydrogenation reaction.[18,19] Cobalt nitrate hexahydrate $Co(NO_3)_2.6H_2O$ was dissolved in 25 ml deionized water to obtain an aqueous solution. Alumina was then mixed in the aqueous solution, stirred and heated continuously, with an increase in temperature of 15 °C every 30 min until the water evaporated and semi-solid slurry remained. The precursor semi-solid slurry was then dried overnight at 105 °C and the dried sample was calcined under an air atmosphere at 750 °C in a furnace for 3 h. The obtained calcined sample was ground and sieved to a particle size range of 50-212 microns. Finally, the sieved catalyst was reduced at 800 °C in a reduction furnace under a H_2 atmosphere (5 % H_2 and 95 % N_2) for 2 h.

In addition, different metal catalysts were studied at optimized conditions to investigate their influence on CH_4 production. The metals investigated were 10 wt.% of Ni, Mo, and Fe

on alumina support and were prepared by wet impregnation method. The metals have all been reported to be effective, to different extents, in the catalytic hydrogenation reaction. [14] Nickel nitrate hexahydrate, iron (III) nitrate nonahydrate, and ammonium molybdate (para) tetrahydrate were used for impregnation with the alumina support. The prepared solutions were dried and calcined at 750 °C. After calcination, the obtained catalysts were ground and sieved to particle size of 50- 212 microns and reduced under H_2 at 800 °C for 2h.

In addition to the Al_2O_3 catalyst support, other support materials, SiO_2 and MCM-41, were investigated to determine the effect of support on CH_4 yield at optimized process parameters. 10 wt.% $Ni.(NO_3)_2.6H_2O$ solution was added to SiO_2 and MCM-41 supports to obtain 10 wt.%Ni/SiO_2 and 10 wt.% Ni/MCM-41 catalyst respectively. The obtained solution was dried overnight and calcined at 550°C for 3h. The calcined catalysts were ground and sieved to a particle size of 50-212 microns and reduced with hydrogen at 800 °C for 2h.

2.3. Pyrolysis-catalytic hydrogenation reactor system. The pyrolysis of the biomass coupled with catalytic hydrogenation was carried out using a two-stage fixed bed reactor system. A schematic diagram of the system is shown in Figure 1. The first stage reactor for the pyrolysis of the biomass was constructed of stainless steel and was 25 cm long x 5 cm diameter. The mass of biomass used was 1.0 g and mass of catalyst was 1.0 g, except where the biomass:catalyst ratio was investigated The catalytic reactor for tar cracking and hydrogenation of the evolved pyrolysis gases was 32 cm long x 2 cm diameter and also constructed of stainless steel. Both reactors were heated and controlled by two separate furnaces and temperature monitored using thermocouples. The carrier gas was N_2 and passed through the reactors continuously. The H_2 for the catalytic hydrogenation of the pyrolysis gases was supplied by a Packard 9200 H_2 generator with a flow rate between 0.0 ml m^{-1} to 70.0 ml $^{-1}$. Water cooled and dry-ice cooled condensers were attached to the output of the reactor system to collect the liquid product. The product gases were collected in a 25 L Tedlar™ gas sample bag. The experimental procedure consisted of preheated the catalyst reactor to the desired catalyst temperature and once the second stage catalyst reactor reached the temperature, the first pyrolysis stage was then heated from ambient temperature to a final temperature of between 500 °C and 800 °C at a heating rate of 20 °C min^{-1} to determine the optimum pyrolysis temperature. Baseline experiments were also carried out using quartz sand in place of the catalyst for comparison. Repeat tests were performed for accuracy and negligible difference was observed between experiments.

2.4. Gas Analysis. The product gases collected in the 25 L Tedlar™ gas sample bag were analysed immediately using a suite of different column gas chromatographs. Hydrocarbon gases were analysed using a Varian CP-3380 column gas chromatograph having a 80-100 mesh HayeSep column of 2m length × 2mm diameter with flame ionization detection and N_2 as carrier gas. Permanent gases, H_2, N_2, O_2, CO_2 and CO were analysed using a Varian CP-3330 having a 60-80 mesh HayeSep column of 2m length × 2mm diameter with thermal conductivity detection and Ar as carrier gas. There was a similar retention time of CO and CO_2 on the column, therefore ,a different VarianCP-3330 gas chromatograph was used for CO_2 analysis equipped with the same column, detector and Ar carrier gas but operated with different chromatographic conditions.

2.5. Catalyst characterization. The BET surface area and BJH pore size of the catalyst were determined by N_2 adsorption experiments using a Tristar 3000 instrument. Metal type and crystal structure were identified using X-ray diffraction (XRD). XRD was carried out using an XPERT X-ray diffractometer having radiation CuKα. Peaks were identified using High Score Plus software package. The particle size of metallic species were calculated by using the High Score Plus software having a built-in program for Scherrer equation calculation. The morphology of the catalysts were studied by Hitachi SU8230 scanning electron microscope (SEM) operating at 20 kV with metal mapping obtained using coupled energy dispersive X-ray spectroscopy (EDXS). Hydrogen-temperature programmed reduction (H_2-TPR) was carried out on the catalyst using a Schimadzu TGA-50 in the presence of hydrogen (5 vol.% H_2 and 95 vol.% N_2) to investigate the effect of calcination temperature on the reducibility of the catalysts.

3. RESULTS AND DISCUSSION

Initial experiments focused on the determination the influence of catalyst temperature and then the influence of biomass pyrolysis temperature in relation to methane yield. For these experiments, the catalyst used was 10 wt.% Co/Al_2O_3 and there was no addition of gaseous H_2 to the 2^{nd} stage reactor. Once the catalyst temperature and pyrolysis temperature which gave the highest CH_4 yield were determined, the catalytic hydrogenation reactions were undertaken with the addition of H_2 gas to the second stage and the range of process parameters and different catalysts were then investigated.

3.1. Influence of catalyst temperature. The influence of catalyst temperature on the product yield and gas composition of the produced gases was undertaken at catalyst temperatures within the range of 300 - 700 °C. The pyrolysis of biomass was maintained at a fixed final temperature of 600 °C and the catalyst used was 10 wt.% Co/Al_2O_3. No H_2 was introduced to the reactor system for these experiments. The results in relation to product yield, gas ratios and gas volumetric composition are shown in Table 2. In addition, Figure 2 shows the gas yield and composition in relation to the mass of biomass. Table 2 show that with the increase in catalyst temperature from 300 - 700 °C the overall gas yield significantly increased from 34.5 wt.% to 66.53 wt.%. There was a consequent decrease in liquid product yield from 34.9 wt.% to 8.36 wt.%, suggesting that the increase in catalyst temperature resulted in cracking of pyrolysis gases.[20] The solid char reflects the residual char from the biomass produced at the pyrolysis temperature of 600 °C, but also some catalyst carbonaceous coke deposits. Table 2 also shows the product yield and gas data for the catalyst 'blank' experiment, where quartz sand at 300 °C was substituted for the Co/Al_2O_3 catalyst. Comparison of the sand and the Co/Al_2O_3 catalyst data at 300 °C showed similar results, but with a higher total gas and solids yield and lower liquid yield. This suggests that the active metal of the catalyst promoted cracking reactions of the pyrolysis gases to produce more gas and less liquid, but also generating more solid deposits as coke on the catalyst.

Figure 2 shows that the CH_4 yield remained at ~1.0 $mmolg^{-1}_{biomass}$ with the increase in catalyst temperature from 300 - 700 °C. Figure 2 also shows that with the increase in temperature, H_2 and CO yield increased with the rise in temperature from 300 - 700 °C, but the CO_2 yield increased up to a catalyst temperature of 600 °C but then reduced at 700 °C. The increase in H_2 and CO_2 with the decrease in liquid yield was because of the cracking of higher hydrocarbons. At lower temperatures i.e. below 600 °C the exothermic water gas shift reaction increased the H_2 yield as indicated by the increase in the H_2/CO ratio and decrease in the CO/CO_2 ratio (Table 2). Also it can be seen that at higher temperatures i.e. above 500 °C there was a rise in CO and decrease in CO_2 and the CO/CO_2 ratio increased, which may be due to the endothermic Boudouard reaction (Table 1, equation 10) as also suggested by Zanzi et al.[21] and Rozas et al.[22]

3.2. Influence of biomass pyrolysis temperature. The influence of final biomass pyrolysis temperature on the CH_4 yield from the pyrolysis-catalytic hydrogenation of biomass was carried out in the temperature range of 500 – 800 °C. The catalyst used in the 2nd stage was 10 wt.% Co/Al_2O_3 and the catalyst temperature was kept constant at 500 °C. No H_2 was

introduced into the reactor system for these experiments. Table 3 shows the product yield, gas composition (vol.%) and the various gas ratios. Figure 3 shows the gas yield in mmol $g^{-1}_{biomass}$. Included in Table 3 are results for quartz sand in place of the Co-Al_2O_3 catalyst as a blank experiment. When the Co-Al_2O_3 catalyst was introduced into the catalyst reactor, there was a marked increase in total gas yield from 32.5 wt.% with sand to 50.2 wt.% with the Co-Al_2O_3 catalyst and a consequent marked decrease in liquid, due to enhanced cracking of the pyrolysis gases in the presence of the catalyst. Table 3 shows that with the increase in the pyrolysis temperature from 500 - 800 °C, the amount of residual char decreased, showing that the biomass continued to degrade at higher pyrolysis temperatures. The solid also includes a small amount of carbonaceous coke deposited on the catalyst. The result of the increased biomass degradation was an increase in the yield of product liquid and a slight increase in product gas yield. Akubo et al.[6] studied the pyrolytic thermal degradation of several different biomass types and the main components of biomass using thermogravimetric analysis up to a final temperature of 800 °C. They showed that the main mass loss of biomass occurred between 250 – 400 °C, but there was a continued smaller loss of mass as the pyrolysis temperature was increased from 400 – 800 °C. The loss of mass at higher temperature was attributed mainly to the presence of lignin in the biomass types, since the thermal decomposition of lignin occurred over a wide temperature range of 280 – 800 °C, whereas cellulose degradation occurred between 320-380 °C and hemicellulose between 250 – 550 °C. Similar results have also been reported by Wang et al.[23] The results here for the waste wood pyrolysis, suggest that the thermal degradation of the biomass at higher temperature is mainly from lignin decomposition.

Table 3 also shows the volumetric gas composition for the product gas produced from the pyrolysis-catalysis of the biomass. The influence of pyrolysis temperature on the volumetric gas composition was small, showing an increase in CH_4, CO and CO_2 and decrease in H_2 and CnHn hydrocarbons with increasing temperature. Figure 3 shows that as the pyrolysis temperature was increased, there was an increase in CH_4, H_2, CO and CO_2 from the biomass (mmol $g^{-1}_{biomass}$). The highest gas yield was for H_2, which increased from 9.6 to 10.5 mmol $g^{-1}_{biomass}$, together with an increase in the CH_4 yield from 0.72 mmol $g^{-1}_{biomass}$ to 1.69 mmol $g^{-1}_{biomass}$ with increased pyrolysis temperature. The CO and CO_2 also increased in yield with increasing pyrolysis temperature. These changes in gas composition are reflected in the gas ratios shown in Table 3. The thermal degradation of the biomass at higher temperatures would release increased H_2, CO, CO_2, CH_4 and other non-oxygenated and oxygenated hydrocarbons leading to a range of cracking, gasification and reforming reactions and influencing the various gas ratios.[24,25]

The influence of final pyrolysis temperature in the 1st stage reactor on the yield of CH_4 showed that the maximum yield of 1.69 mmol $g^{-1}_{biomass}$ was obtained at a final pyrolysis temperature of 800 °C. In addition, the influence of catalyst temperature in the 2nd stage reactor on the yield of CH_4 showed that the maximum yield of 1.2 mmol $g^{-1}_{biomass}$ was obtained at a catalyst temperature of 500 °C. Therefore, to determine the effect of other operating parameters and the investigation of different catalysts on the production of CH_4 from the pyrolysis of biomass coupled with the catalytic hydrogenation of the evolved pyrolysis gases was with a fixed 1st stage, final pyrolysis temperature of 800 °C and a fixed 2nd stage catalyst temperature of 500 °C.

3.3. Influence of hydrogen gas hourly space velocity. The influence of H_2 gas hourly space velocity on CH_4 yield from the pyrolysis-catalytic hydrogenation of biomass was investigated using a 10 wt.% Co/Al_2O_3 catalyst with a final pyrolysis temperature of 800 °C and catalyst temperature of 500 °C. Hydrogen was introduced into the second stage catalyst reactor at different gas flow rates (0.0 – 70.0 ml $min.^{-1}$), reflecting the required H_2 gas hourly space velocities of 0, 600, 1200, 1800, 2400, 3000, 3600 and 4200 ml h^{-1} $g^{-1}_{catalyst}$. Table 4 shows the product yield, gas ratios and gas volumetric composition in relation to H_2 gas hourly space velocity and Figure 4 shows the gas yield and composition in relation to the mass of biomass (mmol $g^{-1}_{biomass}$). Table 4 shows the influence of H_2 space velocity on the product yield in terms of mass of biomass, including the added mass of H_2 used for the hydrogenation reactions, which consequently produced total mass yields of over 100%. The product yield shows that the liquid and gas yield increased with increased addition of H_2 as a result of the production of product water and unreacted H_2 respectively. The added H_2 was involved in the production of product water, and hydrogenation reactions, but also H_2 was produced in reactions, therefore a H_2-free mass balance could not be calculated accurately. The product yield data also shows that the introduction of H_2 to the reaction system caused the reduction of solids from 21.6 wt.% in the absence of H_2 and to 19.0 wt.% at higher levels of H_2 addition. This was due to the interaction of H_2 with the coke on the catalyst to produce CH_4 [26] (Table 1, equation 11). Figure 4 shows the mass of gases (excluding H_2) produced from the biomass (mmol $g^{-1}_{biomass}$). The data shows that in the absence of H_2 addition to the catalyst reactor, the CH_4 yield was 1.68 mmol $g^{-1}_{biomass}$, however, when H_2 was introduced (at 600 ml h^{-1} $g^{-1}_{catalyst}$) there was a significant increase in CH_4 yield to 2.4 mmol $g^{-1}_{biomass}$. An increase in the added H_2 resulted in an increase in CH_4 yield to 5.08 mmol $g^{-1}_{biomass}$ at 3600 ml h^{-1} $g^{-1}_{catalyst}$ H_2 space velocity. Figure 4 also shows that the increase in CH_4 yield was accompanied by a decrease in

CO_2 and CO yield from 5.8 to 1.8 mmol $g^{-1}_{biomass}$ and from 5.07 to 2.9 mmol $g^{-1}_{biomass}$ respectively. Similarly, it can be seen from Table 4 that the CH_4 concentration in the product gas increased from 13.1 to 50.7 vol. % with the increase in H_2 space velocity from 0- 3600 ml h^{-1} $g^{-1}_{catalyst}$. The increase in CH_4/CO_2 and CH_4/CO ratio (Table 4) showed that the addition of H_2 significantly improved the catalytic hydrogenation reaction (Table 1, equations 8 and 9).

Figure 4 also show that at the higher H_2 input of 4200 ml h^{-1} $g^{-1}_{catalyst}$, the CH_4 yield declined to 4.4 mmol $g^{-1}_{biomass}$. Table 4 also shows that the CH_4/CO_2 ratio reduced from 2.76 to 2.38 and the CH_4/CO ratio reduced from 1.74 -1.2 with the increase in H_2 space velocity from 3600 - 4200ml h^{-1} $g^{-1}_{catalyst}$. The decrease in CH_4 yield at the highest H_2 space velocity could be related to the reduced contact time between reactant gases and catalyst which ultimately resulted in lower yield of CH_4. Rahmani et al.,[27] investigated the effect of gas space velocities in the range of 6000-18000 ml $h^{-1}g^{-1}_{catalyst}$ in a fixed bed reactor for the methanation of CO_2 using a Ni/Al_2O_3 catalyst in a fixed bed reactor at 350 °C. They reported that with the increase in gas space velocity, the CO_2 conversion reduced and ultimately resulted in lower CH_4 yield. They reported that the higher gas space velocities result in the reduced contact time between the reactant gases and catalyst resulting in the lower conversion of CO_2. Similar results have been reported by Vita et al.[28] in relation to the effect of gas hourly space velocity in the range of 10000-50000 ml h^{-1} $g^{-1}_{catalyst}$ with Ni-gadolinium-ceria catalysts for CO_2 methanation. They showed that the maximum CH_4 yield was obtained at a gas hourly space velocity of 10000 ml h^{-1} $g^{-1}_{catalyst}$ because of the increased residence time of the reactant gases with the catalyst at that gas space velocity. Aziz et al.,[12] have suggested that non-stoichiometric conditions for the catalytic hydrogenation reaction may be responsible for reduced methanation. They studied the effect of H_2/CO_2 ratio on CH_4 yield using Ni-promoted mesostructured silica nanoparticle catalysts in a fixed bed reactor at 300 °C. They reported that an optimum H_2/CO_2 ratio is required for the catalytic hydrogenation reaction. According to their results, the optimum H_2/CO_2 ratio for CO_2 conversion and CH_4 yield was 4:1. With the increase in ratio from 4:1 to 7:1 a decrease in CO_2 conversion and CH_4 yield was observed. They indicated that the initial enhancement and finally decline of catalytic hydrogenation reaction was because of differences in the amount of H_2 during the reaction. The stoichiometric H_2/CO_2 ratio of 4:1 produces an optimum amount of absorbed H_2 on the catalyst to hydrogenate the carbonated species to convert it into CH_4. Similarly, Rahmani et al.,[27] also studied the effect of H_2/CO_2 ratio using a Ni/Al_2O_3 catalyst with a H_2/CO_2 ratio in the range of 3:1 to 4:1. They reported that a H_2/CO_2 ratio at stoichiometric conditions results in an increase in CO_2 conversion and having no influence on the selectivity of CH_4. However, some studies have reported an increase in CO_2

conversion with an increase in H_2/CO_2 ratio. Lu et al.,[29] studied CO_2 catalytic hydrogenation over NiO supported on SBA-15 (mesoporous silica sieve material) catalyst over the temperature range of 300 - 450 °C in a fixed bed reactor. They reported that at higher H_2/CO_2 ratios above the stoichiometric ratio was favorable for CO_2 conversion and concluded that CO_2 conversion increased with the increase in the H_2/CO_2 ratio. However, at H_2/CO_2 ratios over 6:1, CO_2 conversion remained constant.

3.4. Influence of biomass/catalyst ratio. The influence of biomass/catalyst ratio on the production of methane from the pyrolysis-catalytic hydrogenation of biomass was investigated using the 10 wt.% Co/Al_2O_3 catalyst with a final pyrolysis temperature of 800 °C, catalyst temperature of 500 °C and a fixed nominal H_2 gas hourly space velocity of 3600 ml h^{-1} $g^{-1}_{catalayst}$. The biomass/catalyst ratios of 1:0.5, 1:1, 1:2 and 1:3.5 were investigated with a constant 1.0 g of biomass and varied mass of catalyst. It should be noted that although the H_2 gas hourly space velocity was fixed at 3600 ml h^{-1} $g^{-1}_{catalyst}$, because the catalyst bed depth would vary with the increased mass of catalyst used, that would also affect the H_2 gas hourly space velocity. The influence of biomass/catalyst ratio in terms of product yield, gas ratios and gas volumetric composition are shown in Table 5 and Figure 5 shows the gas yield and composition in relation to the mass of biomass (mmol $g^{-1}_{biomass}$).

Figure 5 shows that the CH_4 yield increased with increased amount of catalyst, CH_4 yield increasing from 2.8 to 7.2 mmol $g^{-1}_{biomass}$ when the biomass:catalyst ratio was raised from 1:0.5 to 1:3.5. The volumetric CH_4 gas concentration in the product gas thereby increased from 56.2 to 82.1 vol.% (Table 5). The data also show that there was a consequent decrease in CO, CO_2 and CnHn yields. This suggests that the increased amount of catalyst resulted in cracking of the CnHn and also the oxygenated and non-oxygenated hydrocarbons produced from the biomass pyrolysis. Other researchers [30,31] investigating the catalytic-pyrolysis of biomass have reported that higher catalyst ratios produce enhanced cracking of hydrocarbons and oxygenated hydrocarbons. In addition, the increased amount of catalyst would result in more active metal sites for increased hydrogenation of the CO and CO_2 (Table 1, equations 8 and 9).

3.5. Influence of metal-Al_2O_3 catalyst type. The influence of four different types of metal-Al_2O_3 catalyst in relation to the production of CH_4 from the pyrolysis-catalytic hydrogenation of biomass was investigated. The metal loading was 10 wt.% to produce Ni-Al_2O_3, Fe-Al_2O_3, Co-Al_2O_3 and Mo-Al_2O_3 catalysts. The experiments were conducted at a final pyrolysis temperature of 800 °C, catalyst temperature of 500 °C and fixed H_2 gas hourly space velocity of 3600 ml h^{-1} $g^{-1}_{catalyst}$. A fixed biomass:catalyst ratio of 1:1 was used to carry

out the experiments. The results are shown in Table 6 in terms of product yield, gas ratios and gas volumetric composition. Experiments were also conducted with quartz sand in place of the catalyst for comparison.

Table 6 shows that in the total gas yield was increased with the introduction of metal catalyst compared to sand. It should again be noted that the mass yields are expressed in terms of biomass and do not include the mass of added H_2 gas. Liquid yields were also influenced by the presence of the catalyst, since the added hydrogen was involved in the production of product water (but also hydrogenation reactions and also H_2 production reactions). The results show that total gas yield was influenced by the type of catalyst used, but the composition of the product gas was markedly different. For example, the volumetric gas composition (H_2 free basis) showed that the highest CH_4 gas yield of 66.9 vol.%, was produced with the produce Ni-Al_2O_3 catalyst whilst the Fe-Al_2O_3 and Mo-Al_2O_3 catalysts produced a gas with high concentrations of CO.

Figure 6 shows the gas yield and composition in relation to the mass of biomass (mmol $g^{-1}_{biomass}$). The data shows that the maximum CH_4 yield (6.4 mmol $g^{-1}_{biomass}$) in terms of the mass of biomass was obtained with the Ni/Al_2O_3 catalyst as compared to sand in place of the catalyst, where CH_4 yield was low. The Ni/Al_2O_3 catalyst also exhibited the highest CH_4/CO_2 ratio (3.6) and CH_4/CO ratio (5.05) reflecting the effective catalyst activity for catalytic hydrogenation of CO_2 and CO produced from the biomass. In comparison, the Co-Al_2O_3 catalyst also showed good activity towards CO_2 and CO catalytic hydrogenation with a high CH_4 yield of 5.08 mmol $g^{-1}_{biomass}$ and high CH_4/CO_2 and CH_4/CO ratios (2.76 and 1.74 respectively). However, the Fe-Al_2O_3, and Mo-Al_2O_3 catalysts showed selectivity towards CH_4 production by catalytic hydrogenation. Therefore, among the different metal catalysts studied the activity of the catalysts for CH_4 production decreased in the order Ni>Co>Mo>Fe>Sand. The low catalytic activity for the catalytic hydrogenation reaction shown by the Fe-Al_2O_3, and Mo-Al_2O_3 catalysts suggests that most of the H_2 passed over the catalyst unreacted resulting in increased in overall gas yield and decrease in liquid yield because of low formation of water by the catalytic hydrogenation reaction.

Aziz et al.,[32] studied the influence of different metals promoted on mesostructured silica nanoparticles in a fixed bed reactor for CO_2 catalytic hydrogenation using CO_2 and H_2 as reactant gases. The catalytic activity of the studied metals catalyst decreased in the order Rh> Ru>Ni>Ir>Fe>Cu at 350 °C catalyst temperature. They reported that Rh, Ru and Ni were active for CO_2 catalytic hydrogenation even at low temperature, but Fe, Ir and Cu required high temperature for CO_2 catalytic hydrogenation. Yan et al.,[33] studied the effect of various

transition metal loadings with a Ni/MgO catalyst for CO_2 catalytic hydrogenation. They showed that at a catalyst temperature of 350 °C, the addition of Co and W resulted in an increase in catalyst activity but with the addition of Fe and Mo, the CO_2 conversion decreased. The literature have also reported that amongst the transition metals, Ni based catalysts are effective for carbon oxide catalytic hydrogenation, whilst Fe-based and Mo-based catalysts are not. It has been reported that Fe-catalysts have high activity while Mo-catalysts have low activity for the methane production via the COx methanation process.[34] In this work, a high yield of CO was produced from Fe and Mo based Al_2O_3 catalysts. In the case of Fe a possible reason for the decrease in CH_4 yield with enhanced CO production is the promotion of the reverse water gas shift (RWGS) reaction.[35] But in the case of Mo/Al_2O_3, the Al_2O_3 support itself has some catalytic activity and can crack the higher hydrocarbons into CO_x,[36] which in the absence of non-active metal the CO_x does not react with H_2 and passes through the catalytic bed unreacted and resulted in higher percentage in the output gaseous mixture.

Ni-based and Co-based catalysts have been shown to be active in different reaction systems. For example, Hu and Lu [37] examined the catalytic steam reforming of acetic acid and reported increased syngas yield with Ni and Co catalysts could be attributed to their high catalytic hydrogenation activity up to 623 °C. They also reported that Co and Ni catalyst have the ability to crack C-C and C-H bonds which enhanced their activity, however Fe can only crack C-C bonds. They ranked the catalytic activity for different transition metals in the order Ni>Co>Fe>Cu. Similarly, Chen et al.,[38] studied the effect of Ni, Co, Ba and Cu with Fe_2O_4 for the reforming of toluene for syngas production at 850°C. They showed that the highest catalytic activity for toluene decomposition was shown by Ni followed by Co, Ba and Cu.

3.6. Influence of catalyst calcination temperature. The influence of calcination temperature in the preparation of the 10 wt.% Ni/Al_2O_3 catalyst in relation to the production of methane from the pyrolysis-catalytic hydrogenation of biomass was investigated. Catalyst calcination temperatures of 550, 650, 750 and 850 °C were investigated. The prepared catalysts were characterised in terms of their surface area and porosity using N_2 adsorption-desorption isotherms. Table 7 shows the results of the surface area and porosity in relation to the calcination temperature of the 10 wt.% Ni/Al_2O_3 catalysts, which shows that an increase in calcination temperature results in a significant decrease in surface area of the catalyst, accompanied by an increase in pore sizes. Zhang et al.,[39] have similarly shown that increasing the catalyst preparation calcination temperature for a Ni/Al_2O_3 catalyst from 500 -1000 °C a significant decrease in catalyst surface area from 196.2- 67.3 $m^2\ g^{-1}$ was observed. Hydrogen-

temperature programmed reduction (H_2-TPR) using a TGA was performed to investigate the effect of calcination temperature on the reducibility of metals oxide (NiO) into metals (Ni). The results are shown in Figure 7. The highest weight loss was observed with the 10 wt.% Ni/Al_2O_3 catalyst calcined at 550 ^oC while the lowest weight loss was exhibited by the 10 wt.% Ni/Al_2O_3 catalyst calcined at 850 ^oC. It was observed that the catalyst calcined at 550 ^oC started reducing at lower temperature compared to the catalyst calcined at higher temperatures. Therefore, it may be concluded that with the increase in calcination temperature the interaction between the metal and support becomes more stronger and it becomes difficult to reduce the catalyst calcined at higher temperature. Daroughegi et al.,[40] also reported on the increase in calcination temperature of a 25 wt.% Ni/Al_2O_3 catalyst from 500 - 800 ^oC in relation to metal-support interaction. They showed that a reduction peak in the temperature range from 500-700 ^oC corresponded to the reduction of strongly interacted metal and the support while, a reduction peak at 800 ^oC corresponded to the reduction of nickel aluminate. They also reported that with increase in calcination temperature the interaction between metal and support became stronger.

The prepared catalysts were investigated for their influence on the production of methane during the pyrolysis-catalytic hydrogenation of biomass. The results are shown in Table 8 in terms of gas composition and Figure 8 shows the gas yield from the biomass. The pyrolysis final temperature was 800 °C, catalyst temperature was 500 °C and H_2 gas space velocity was 3600 ml h^{-1} $g^{-1}_{catalyst}$. Biomass/catalyst ratio of 1:1 was used to carry out the experiments. Table 8 shows that the volumetric CH_4 concentration decreased from 75.5 to 57.8 vol.% and the CH_4 yield decreased from 7.4 – 5.8 mmol $g^{-1}_{biomass}$ (Figure 8). The results show that the catalytic activity for CH_4 production decreased with the increase in calcination temperature, coinciding with decreased catalyst surface area. The C_nH_n hydrocarbons increased with catalysts prepared at higher temperatures suggesting the catalyst was less effective in cracking the hydrocarbons. Also, the CO and CO_2 increased at higher catalyst calcination temperatures, suggesting that the added H_2 was less effective in the hydrogenation of these carbon oxides. This was also reflected in the CH_4/CO and CH_4/CO_2 ratios. Liu et al.,[41] have also reported that increaserd catalyst calcinarion temperature results in lower catalyst activity which was attributed to metal particle (nickel) sintering.

3.7. Influence of catalyst nickel loading. The influence of the amount of Ni metal loading on the alumina support was investigated using nickel loadings of 5, 10 and 15 wt.% of nickel. The prepared catalysts were examined by SEM with EDXS metal mapping to investigate the distribution of Ni on the alumina support and also by XRD. The results for

SEM-EDXS are shown in Figure 9. The images and data show that the nickel metal is uniformly distributed over the 5 wt.% and 10 wt.% Ni loaded alumina catalysts but for the 15 wt.% Ni loading, there is an obvious increase in nickel particle size, along with a non-uniform distribution. Analysis of the prepared catalyst by XRD (Figure 10) was also used to investigate the particle size (crystallite size) of the different Ni loadings calculated using the Scherrer equation. The results were that the Ni particle size increased from 3.8 nm to 10 nm with the increase in Ni loadings from 5- 15 wt.%. Therefore, it may be concluded that an increase in Ni loading results in metal sintering and results in the increase in particle size of metallic species. Figure 9 shows that the 5 wt.% and 10 wt.% Ni loading, there was uniform dispersion of Ni on the support however with the increase in metal loading to 15 wt.%, Ni particles started to agglomerate evidenced by the appearance of Al_2O_3 peaks. The 5 wt.% and 10 wt.% Ni loading catalysts showed only two visible peaks of Al_2O_3, at the diffraction angles of 45.5° and 66.42°. However, when the Ni loading was further increased to 15 wt.%, four visible Al_2O_3 peaks were observed at diffraction angles of 19.14º, 45.5°, 60.34° and 66.42° possibly because of agglomeration/sintering of Ni particles and non-uniform nickel dispersion.

The effect of the amount of Ni metal loading on alumina support in relation to CH_4 production from biomass was investigated. The final pyrolysis temperature was 800 °C, catalyst temperature was 500 °C and H_2 gas space velocity was 3600 ml h^{-1} $g^{-1}_{catalyst}$. The results are shown in Table 9 for the gas composition and in Figure 11 for the gas yield (mmol $g^{-1}_{biomass}$). The results show that the increase in Ni loading from 5 wt.% to 10 wt.% resulted in an increase in CH_4 yield from 4.4 to 7.4 mmol $g^{-1}_{biomass}$ (Figure 11) and volumetric gas concentration increased from 58.1 to 75.5 vol.% (Table 9), linked to the uniform dispersion of Ni on the alumina support. But, with the further increase in Ni loading up to 15 wt.% the CH_4 yield decreased to 5.0 mmol $g^{-1}_{biomass}$ and 66.0 vol.%. Also, the highest CH_4/CO_2 ratio was observed with the 10 wt.% Ni/Al_2O_3 catalyst. In addition, the maximum conversion of CnHn was also observed with the 10 wt.% Ni/Al_2O_3 catalyst. The low CH_4 selectivity for the 5 wt.% Ni/Al_2O_3 catalyst suggests insufficient Ni on the alumina support and the reduced selectivity for the 15 wt.% Ni/Al_2O_3 catalyst was due to sintering of the Ni metal particles and non-uniform distribution.

The influence of the amount of catalyst metal on Ni/F-SBA-15 catalysts with Ni loadings of 1, 3, 5 and 10 wt.% in relation to CO_2 catalytic hydrogenation was investigated by Bukhari et al.[42] They reported that low Ni loading reduced the effectiveness of the catalyst due to insufficient active metal. However, increased Ni loading produced optimum conversion of CO_2 to CH_4 due to the presence of Ni metal and strong metal support interaction. But, at higher

Ni loading, CO_2 conversion decreased which was attributed to sintering of metal and resulted in weaker metal support interaction.

3.8. Influence of catalyst support material. Three different catalyst support materials, Al_2O_3, MCM-41 and SiO_2, each loaded with 10 wt.% Ni were investigated to determine the influence on CH_4 production from biomass by pyrolysis-catalytic hydrogenation. Initial characterization to investigate the morphology of the catalysts was carried out using SEM with EDXS metal mapping (Figure 12). A uniform distribution of small Ni particles was observed over the surface of the Al_2O_3 support, however, for the MCM-41 and SiO_2 support materials, larger Ni particles and non-uniform distribution of the NI can be seen due to metal sintering. The crystal structure and particle size of the Ni with the different support materials were investigated by XRD. Figure 13 shows the presence of metallic Ni at diffraction angles of 2theta at 44.3°, 51.68° and 76.24° for all of the supports and the intensity of Ni diffraction peak increased in the order Al_2O_3<MCM-41<SiO_2. The crystallite particle size of the Ni metal species was determine using the Scherrer equation and was found to be 8.3 nm for Al_2O_3, 13.3 nm for MCM-41 and 17.6 nm for SiO_2.

The influence of the 10 wt.% Ni loaded Al_2O_3, MCM-41 and SiO_2, supports in relation to CH_4 production from biomass were investigated. The final pyrolysis temperature was 800 °C, catalyst temperature 500 °C with H_2 gas space velocity at 3600 ml h^{-1} $g^{-1}_{catalyst}$ and biomass:catalyst ratio of 1:1Table 10 shows the product gas composition and Figure 14, the gas yield. The highest CH_4 yield of 7.4 mmol $g^{-1}_{biomass}$ was obtained with the Al_2O_3 support material followed by MCM-41 at 4.3 mmol $g^{-1}_{biomass}$ and SiO_2 with 3.0 mmol $g^{-1}_{biomass}$. Also, maximum CH_4 gas concentration followed the same order at Al_2O_3>MCM-41>SiO_2 with 75.5, 58.4 and 31.4 vol. % concentrations respectively. The CH_4/CO_2 and CH_4/CO ratios of the Al_2O_3 catalyst also reflected the higher conversion of CO_2 and CO by catalytic hydrogenation. The increased selectivity towards CH_4 production clearly linked to the lower Ni particle size and uniform distribution of the Al_2O_3, catalyst compared with the MCM-41 and SiO_2 catalysts.

Du et al.,[43] studied the effect of effect of MCM-41 for CO_2 catalytic hydrogenation and they found very low activity of the MCM-41 support. According to Frontera et al.,[43] the reason for the lower activity reported by Du et al.,[44] with MCM-41 was because of the lower stability of MCM-41 in the presence of water vapour. Aziz et al.,[45] investigated the influence of the presence of water vapours during CO_2 catalytic hydrogenation using a 5 wt.% Ni/ MSN (mesostructured silica nanoparticles) catalyst. They reported that the presence of water vapour results in the decrease in carbonyl species, a major intermediate product for CH_4 production by

CO_2 hydrogenation. Also, it has been reported that presence of water favors the sintering of nickel on the mesostructured silica nanoparticle support and results in the decreased catalytic activity.

Overall the results have shown that a maximum CH_4 yield of 7.4 mmol $g^{-1}_{biomass}$ and maximum CH_4 gas composition of 75.5 vol.% was obtained from the pyrolysis-catalytic hydrogenation of biomass. The optimised process conditions were obtained using a 10 wt.% Ni supported on Al_2O_3 catalyst prepared at a calcination temperature of 550 °C and with a biomass final pyrolysis temperature of 800 °C, catalyst temperature of 500 °C and H_2 gas hourly space velocity of 3600 ml h^{-1} $g^{-1}_{catayst}$. The results may be compared with our previous work [46] that investigated the influence of various process parameters on the catalytic hydrogenation of CO_2. The maximum CH_4 yield, maximum CO_2 conversion and CH_4 selectivity was obtained at 360 °C with an H_2:CO_2 ratio of 4:1 and total gas hourly space velocity of 6000 ml h^{-1} $g^{-1}_{catalyst}$ and reactant gases hourly space velocity of 3000 ml h^{-1} $g^{-1}_{catalyst}$. The maximum CO_2 conversion obtained was 84 mol.% with 81 mol.% CH_4 selectivity and methane yield of 10.8 mmol over a 10 wt.% Ni/Al_2O_3 catalyst. Others have also investigated catalytic hydrogenation of CO_2. For example, Li et al.,[47] studied the catalytic hydrogenation of CO_2 to CH_4 in a fixed bed reactor using a monolithic Ni/Al_2O_3 catalyst at 320 °C with a GHSV of 5000 h^{-1} and pressure of 0.1 MPa. Approximately 90 % of CO_2 conversion was obtained with around 99.9% of methane selectivity. Similarly, Li et al.,[48] studied the CO_2 methanation reaction using H_2 and CO_2 as feed gases in molar ratio of 4:1. Experiments were carried out in a pressurized environment of 3 MPa and gas hourly space velocity of 3600 ml $h^{-1}g^{-1}$. They used Ni/ZrO_2 as a catalyst. The maximum CO_2 conversion obtained was 92.5 % with 99.9 % of CH_4 selectivity.

There is less work on the catalytic hydrogenation of other more complex feedstocks such as biomass or bio-gas. Zhang et al.,[49] studied the simultaneous tar reforming and catalytic hydrogenation of syngas produced from biomass using a Ni/olivine-CaO catalyst. The maximum CH_4 concentration obtained was 26.9 vol.%. Kienberger et al.,[50] also used the product gas from the fluidised bed gasification of biomass as feedstock with a separate methanation reactor with Ni/MgO-SiO_2 as a catalyst. They reported that at a GHSV of 1000 h^{-1} and at a temperature of 260 °C the maximum methane yield of 33.7 vol.% was obtained.

Several modelling studies have investigated the conversion of biomass to CH_4 via gasification and catalytic hydrogenation. For example, Vakalis et al.,[51] thermodynamically modelled a biomass gasifiier with a down stream methanation/reforming reactor to react the gasification product gas with input H_2. The optimal ratio of biomass gasification product gas

to input hydrogen was identified at 1:0.9 which produced a molar fraction of CH_4 of 40%. Van der Meijden et al.,[52] used Aspen Plus® to model three biomass gasification systems with downstream methanation to identify the optimal process to enhance the CH_4 production. They reported that methane concentration in the output gaseous mixture reached ~90% after gas purification (removal of CO_2 and H_2O). Duren et al., [53] used BELSIM-VALI® model to investigate upgrading of biomass gasification product gas to CH_4. They reported a maximum calculated CH_4 concentration of 54.8 vol.% at the exit of the methanation reactor.

The interest demonstrated in the literature suggests that there is potential in the process of methane production from biomass, via pyrolysis-catalytic hydrogenation. Pyrolysis of biomass would produce a bio-char suitable for use as a soil improver coupled with catalytic hydrogenation of the product pyrolysis carbon oxide gases to produce methane. However, manipulating the product gas composition that enters the catalytic hydrogenation reactor would be advantageous. For example, through the use of catalysts in an additional reactor stage to crack the heavy hydrocarbons from pyrolysis. In addition, also providing a sustainable source for the hydrogen, such as from biomass, would significantly improve the attractiveness of the process. The goal of producing sustainable methane as a substitute natural gas has an added economic incentive because of the already existing infrastructure for natural gas in many countries.

4. CONCLUSIONS

A detailed operating parametric study and catalytic investigation has been undertaken into the production of CH_4 from the catalytic hydrogenation of biomass. The results have shown that:

A suitable catalyst temperature is required to enhance the CH_4 yield. The maximum CH_4 yield was obtained with a catalyst temperature of 500 °C. Above this temperature, the produced CH_4 reacts with autogenerated water to enhance the steam reforming reaction and converts the CH_4 into H_2 and CO. However, lower temperatures favor hydrocarbon production because of poor cracking of higher hydrocarbons. An optimized temperature for the pyrolysis stage is required to decompose the biomass completely. For the particular biomass sample (wood pellets) used here, a final pyrolysis temperature of 800 °C was found to produce the highest level of biomass decomposition. This was linked to the higher temperatures required to decompose the lignin component of the biomass. Increasing the biomass:catalyst ratio from 1:0.5 to 1:3.5 produced enhanced CH_4 yield due to the increased. With the increase in catalyst

quantity, the CH_4 yield increased the cracking of hydrocarbons and catalytic hydrogenation. The influence of varying the H_2 gas space velocity showed that an optimum H_2 input was required, increasing H_2 produced enhanced hydrogenation of CO and CO_2 and higher CH_4 yield. However, at higher H_2 input, CH_4 yield reduced with the increase in CO_2 possibly because of the disturbance in stoichiometric ratios. Among the different metal catalysts studied the maximum catalytic activity was shown by the nickel based catalyst. The CH_4 production decreased in the order Ni>Co>Mo>Fe. Higher Ni/Al_2O_3 catalyst preparation calcination temperature reduced CH_4 production, linked to lower catalyst surface area and increased sintering of the Ni metal crystallites at higher temperature. A suitable amount of Ni metal loading was required to enhance the hydrocarbon and oxygenated hydrocarbon cracking and catalytic hydrogenation reactions simultaneously. With the increase in catalyst loading from 5 wt.% to 10 wt.% the CH_4 yield increased, however, with the further increase in metal loading to 15 % the CH_4 yield decreased. SEM-EDXS and XRD analysis of the catalysts indicated that increased metal loading leading to Ni particle sintering and non-uniform distribution of metallic Ni and a consequent decrease in catalytic activity. Among the different support materials investigated, the maximum catalytic activity was shown by the Al_2O_3 support. While the decrease in catalytic activity was observed with MCM-41 and SiO_2. SEM-EDXS and XRD characterisation of the catalysts showed smaller Ni crystallite size and a more uniform Ni distribution for the Ni/Al_2O_3 catalyst compared with the Ni/MCM-41 and Ni/SiO_2 supported catalysts.

REFERENCES

1. Ayalur Chattanathan, S., Adhikari S., Abdoulmoumine N. A review on current status of hydrogen production from bio-oil. Renew Sust Energ Rev 2012;16(5):2366-2372.
2. Kan, T., V. Strezov and T.J. Evans, Lignocellulosic biomass pyrolysis: A review of product properties and effects of pyrolysis parameters. Renew Sust Energ Rev 2016;57:1126-1140.
3. Hosseini, S.E., Wahid M.A., Ganjehkaviri A. An overview of renewable hydrogen production from thermochemical process of oil palm solid waste in Malaysia. Energ Convers Manage 2015;94:415-429.
4. Bridgwater, A.V., Review of fast pyrolysis of biomass and product upgrading. Biomass Bioenerg 2012;38:68-94.
5. Zhang, W., Automotive fuels from biomass via gasification. Fuel Proc Technol 2010;91(8):866-876.
6. Akubo, K., Nahil M.A., Williams P.T. Pyrolysis-catalytic steam reforming of agricultural biomass wastes and biomass components for production of hydrogen/syngas. J Energy Inst 2018 (doi.org/10.1016/j.joei.2018.10.013)
7. Ye, M., Tao Y., Jin F., Ling H., Wu C., Williams P.T., Huang J. Enhancing hydrogen production from the pyrolysis-gasification of biomass by size-confined Ni catalysts on acidic MCM-41 supports. Catal Today 2018;307:154-161.
8. Keefer, B.G., Babicki M.L., Sellars B.G., Ng E. Method and system for biomass hydrogasification. 2016, Google Patents, US20130023707A1.
9. Ogden, J., Jaffe A.M., Scheitrum D., McDonald Z., Miller M. Natural gas as a bridge to hydrogen transportation fuel: Insights from the literature. Energ Policy 2018;115:317-329.
10. Li, W.; Wang H.; Jiang X.; Zhu J.; Liu Z.; Guo X.; Song C. A short review of recent advances in CO_2 hydrogenation to hydrocarbons over heterogeneous catalysts. RSC Adv 2018;8(14):7651-7669.
11. Muroyama, H., Tsuda Y., Asakoshi T., Masitah H., Okanishi T., Matsui T., Eguchi K. Carbon dioxide methanation over Ni catalysts supported on various metal oxides. J Catal 2016;343:178-184.
12. Aziz, M.A.A., Jalil A.A., Triwahyono S., Mukti R.R., Taufiq-Yap Y.H., Sazegar M.R. Highly active Ni-promoted mesostructured silica nanoparticles for CO_2 methanation. Appl Catal B 2014;147:359-368.
13. Stangeland, K.; Kalai D.Y.; Li H.; Yu Z. Active and stable Ni based catalysts and processes for biogas upgrading: The effect of temperature and initial methane concentration on CO_2 methanation. Appl Energ 2018;227:206-212
14. Wang, W., Gong J. Methanation of carbon dioxide: an overview. Front Chem Sci Eng 2011;5:2-10.
15. Ma, S., Song W., Liu B., Zheng H., Deng J., Zhong W., Liu J., Gong X.Q., Zhao Z. Elucidation of the high CO_2 reduction selectivity of isolated Rh supported on TiO_2: a DFT study. Catal Sci Technol 2016;6:6128-6136.

16. Wierzbicki, D.; Debek R.; Motak M.; Grzybek T.; Gálvez M.E.; Da Costa P. Novel Ni-La-hydrotalcite derived catalysts for CO_2 methanation. Catal. Comm. 2016;83:5-8.

17 He, L., Q. Lin, Y. Liu, and Y. Huang, Unique catalysis of Ni-Al hydrotalcite derived catalyst in CO2 methanation: cooperative effect between Ni nanoparticles and a basic support. Journal of Energy Chemistry, 2014. **23**(5): 587-592.

18. Razzaq, R.; Li C.; Usman M.; Suzuki K.; Zhang S. A highly active and stable Co_4N/γ-Al_2O_3 catalyst for CO and CO_2 methanation to produce synthetic natural gas (SNG). Chem Eng J 2015;262:1090-1098.

19. Fischer, F., Tropsch H., Dilthey P. Reduction of carbon monoxide to methane in the presence of various metals. Brennst Chem 1925;6:265-271.

20. Xie, Q., Kong S., Liu Y., Zeng H. Syngas production by two-stage method of biomass catalytic pyrolysis and gasification. Bioresource Technol 2012;110:603-609.

21. Zanzi, R., Sjöström K., Björnbom E. Rapid pyrolysis of agricultural residues at high temperature. Biomass Bioenerg 2002;23(5):357-366.

22. Rozas, R., Escalona N., Sepúlveda C., Leiva K., Chimentão R.J., Garcia R., Fierro J.L.G. Catalytic gasification of pine-sawdust: Effect of primary and secondary catalysts. J Energy Inst 2019 (doi.org/10.1016/j.joei.2019.01.002)

23. Wang, G., Li, W. Li B., Chen H. TG study on pyrolysis of biomass and its three components under syngas. Fuel 2008;87(4):552-558.

24. Shen, Y., D. Ma, X.J.S.E. Ge, and Fuels, CO_2-looping in biomass pyrolysis or gasification. 2017. **1**(8): 1700-1729.

25. French, R. and S. Czernik, Catalytic pyrolysis of biomass for biofuels production. Fuel Processing Technology, 2010. **91**(1): 25-32.

26. Figueiredo, J.L., Bernardo C.A., Chludzinski J.J., Baker R.T.K. The reversibility of filamentous carbon growth and gasification. J Catal 1988;110(1):127-138.

27. Rahmani, S., Rezaei M. Meshkani F. Preparation of highly active nickel catalysts supported on mesoporous nanocrystalline γ-Al_2O_3 for CO_2 methanation. J Ind Eng Chem 2014;20(4):1346-1352.

28. Vita, A., Italiano C., Pino L., Frontera P., Ferraro M., Antonucci V. Activity and stability of powder and monolith-coated Ni/GDC catalysts for CO_2 methanation. Appl Catal B 2018;226:384-395.

29. Lu, B., Kawamoto K. Preparation of the highly loaded and well-dispersed NiO/SBA-15 for methanation of producer gas. Fuel 2013;103:699-704.

30. Tan, Y.L., Abdullah A.Z., Hameed B.H. Catalytic fast pyrolysis of durian rind using silica-alumina catalyst: Effects of pyrolysis parameters. Bioresource Technol 2018;264:198-205.

31. Naqvi, S.R., Uemura, Y., Yusup S.B. Catalytic pyrolysis of paddy husk in a drop type pyrolyzer for bio-oil production: The role of temperature and catalyst. J Anal Appl Pyrolysis 2014;106:57-62.

32. Aziz, M.A.A., Jalil A.A., Triwahyono S., Sidik S.M. Methanation of carbon dioxide on metal-promoted mesostructured silica nanoparticles. Appl Catal A 2014;486:115-122.

33. Yan, Y., Dai Y., He H., Yu Y., Yang Y. A novel W-doped Ni-Mg mixed oxide catalyst for CO_2 methanation. Appl Catal B 2016;196:108-116.

34. Gao, J., Q. Liu, F. Gu, B. Liu, Z. Zhong, and F. Su, Recent advances in methanation catalysts for the production of synthetic natural gas. RSC Advances, 2015. **5**(29): 22759-22776.

35. Kharaji, A.G., A. Shariati and M.A. Takassi, A Novel γ-Alumina Supported Fe-Mo Bimetallic Catalyst for Reverse Water Gas Shift Reaction. Chinese Journal of Chemical Engineering, 2013. **21**(9): 1007-1014.

36. Yorgun, S. and Y.E. Şimşek, Catalytic pyrolysis of Miscanthus×giganteus over activated alumina. Bioresource Technology, 2008. **99**(17): 8095-8100.

37. Hu, X., Lu G. Comparative study of alumina-supported transition metal catalysts for hydrogen generation by steam reforming of acetic acid. Appl Catal B 2010;99: 289-297.

38. Chen, J., Zhao K., Zhao Z., He F., Huang Z., Wei G. Identifying the roles of MFe_2O_4 (M=Cu, Ba, Ni, and Co) in the chemical looping reforming of char, pyrolysis gas and tar resulting from biomass pyrolysis. Int J Hydrogen Energy 2019;44(10):4674-4687.

39. Zhang, C., Hu X., Zhang Z., Zhang L., Dong D., Gao G., Westerhof R., Syed-Hassan S.S.A. Steam reforming of acetic acid over Ni/Al_2O_3 catalyst: Correlation of calcination temperature with the interaction of nickel and alumina. Fuel, 2018. 227: 307-324.

40. Daroughegi, R., F. Meshkani and M. Rezaei, Enhanced activity of CO_2 methanation over mesoporous nanocrystalline $Ni–Al_2O_3$ catalysts prepared by ultrasound-assisted co-precipitation method. International Journal of Hydrogen Energy, 2017. **42**(22): 15115-15125.

41. Liu, X., Yang X., Liu C., Chen P., Yue X., Zhang S. Low-temperature catalytic steam reforming of toluene over activated carbon supported nickel catalysts. J Taiwan Inst Chem Eng 2016;65:233-241.

42. Bukhari, S.N., Chong C.C., Setiabudi H.D., Ainirazali N., Aziz M.A.A., Jalil,A.A., Chin S.Y. Optimal Ni loading towards efficient CH_4 production from H_2 and CO_2 over Ni supported onto fibrous SBA-15. Int J Hydrogen Energ 2019;44:7228-7240

43. Du, G., Lim S. Yang Y., Wang C., Pfefferle L., Haller G.L. Methanation of carbon dioxide on Ni-incorporated MCM-41 catalysts: The influence of catalyst pretreatment and study of steady-state reaction. J Catal 2007;249:370-379.

44. Frontera, P., Macario A., Ferraro M., Antonucci P. Supported catalysts for CO_2 methanation: A review. Catalysts 2017;7:59; doi:10.3390/catal7020059

45. Aziz, M.A.A., Jalil, A.A., Triwahyono, S., Saad M.W.A., CO_2 methanation over Ni-promoted mesostructured silica nanoparticles: Influence of Ni loading and water vapor on activity and response surface methodology studies. Chem Eng J 2015;260:757-764.

46. Jaffar, M.M., Nahil M.A., Williams P.T., Parametric study of CO_2 methanation for synthetic natural gas production (Submitted to Energ. Technol., 2019)

47. Li, Y., Q. Zhang, R. Chai, G. Zhao, Y. Liu, Y. Lu, and F.J.A.J. Cao, *Ni-*Al_2O_3*/Ni-foam* catalyst with enhanced heat transfer for hydrogenation of CO_2 to methane. 2015. **61**(12): 4323-4331.

48. Li, W., X. Nie, X. Jiang, A. Zhang, F. Ding, M. Liu, Z. Liu, X. Guo, and C. Song, ZrO_2 support imparts superior activity and stability of Co catalysts for CO_2 methanation. Applied Catalysis B: Environmental, 2018. **220**: 397-408.

49. Zhang, J., G. Wang and S. Xu, Simultaneous Tar Reforming and Syngas Methanation for Bio-Substitute Natural Gas. Industrial & Engineering Chemistry Research, 2018. **57**(32): 10905-10914.
50. Kienberger, T., C. Zuber, K. Novosel, C. Baumhakl, and J. Karl, Desulfurization and in situ tar reduction within catalytic methanation of biogenous synthesis gas. Fuel, 2013. **107**: 102-112.
51. Vakalis, S., D. Malamis and K. Moustakas, Thermodynamic modelling of an onsite methanation reactor for upgrading producer gas from commercial small scale biomass gasifiers. Journal of Environmental Management, 2018. **216**: 145-152.
52. van der Meijden, C.M., H.J. Veringa and L.P.L.M. Rabou, The production of synthetic natural gas (SNG): A comparison of three wood gasification systems for energy balance and overall efficiency. Biomass and Bioenergy, 2010. **34**(3): 302-311.
53. Duret, A., C. Friedli and F. Maréchal, Process design of Synthetic Natural Gas (SNG) production using wood gasification. Journal of Cleaner Production, 2005. **13**(15): 1434-1446.

FIGURE CAPTIONS

Figure 1. Schematic diagram of the two-stage pyrolysis-catalytic hydrogenation fixed bed reactor.

Figure 2. Influence of catalyst temperature on gas composition from the pyrolysis-catalysis of waste wood (pyrolysis temperature, 600 °C).

Figure 3 Influence of pyrolysis temperature on gas composition during pyrolysis-catalysis of waste wood (catalyst temperature; 500 °C).

Figure 4. Influence of hydrogen gas hourly space velocity on gas composition from the pyrolysis-catalytic hydrogenation of waste wood with 10 wt.% Co/Al_2O_3 catalyst (final pyrolysis temperature of 800 °C and catalyst temperature of 500 °C).

Figure 5. Influence of biomass:catalyst ratio on the gas yield from the pyrolysis-catalytic hydrogenation of waste wood with 10 wt.% Co/Al_2O_3 catalyst (final pyrolysis temperature of 800 °C, catalyst temperature of 500 °C and H_2 space velocity 3600 ml h^{-1} $g^{-1}_{catalyst}$).

Figure 6. Influence of 10 wt.% Ni-Al_2O_3, Fe-Al_2O_3, Co-Al_2O_3 and Mo-Al_2O_3 catalysts on the gas yield from the pyrolysis-catalytic hydrogenation of waste wood (final pyrolysis temperature of 800 °C, catalyst temperature of 500 °C and H_2 gas hourly space velocity of 3600 ml h^{-1} $g^{-1}_{catayst}$).

Figure 7. H_2-TPR of various 10 wt. % Ni/Al2O3 catalysts calcined at different calcination temperatures.

Figure 8. Influence of calcination temperature for the 10 wt.% Ni/Al_2O_3 catalyst preparation on the gas yield from the pyrolysis-catalytic hydrogenation of waste wood (final pyrolysis temperature of 800 °C, catalyst temperature of 500 °C and H_2 gas hourly space velocity of 3600 ml h^{-1} $g^{-1}_{catayst}$).

Figure 9. SEM-EDXS mapping of different nickel loadings on alumina support (a) 5 wt.%-Ni/Al_2O_3 (b) 10 wt.%/Al_2O_3Ni (c) 15 wt.%-Ni/Al_2O_3

Figure 10. XRD patterns of various Ni loadings on Al_2O_3 support.

Figure 11. Influence of Ni metal loading on Ni/Al_2O_3 catalyst on the gas yield from the pyrolysis-catalytic hydrogenation of waste wood (final pyrolysis temperature of 800 °C, catalyst temperature of 500 °C and H_2 gas hourly space velocity of 3600 ml h^{-1} $g^{-1}_{catayst}$).

Figure 12. SEM- with EDX nickel mapping patterns of different catalyst support materials (a) 10 wt.% Ni/SiO_2 (b) 10 wt.% Ni/MCM-41 (c) 10 wt.% Ni/Al_2O_3.

Figure 13. XRD patterns of Ni catalyst with different supports.

Figure 14. Influence of 10 wt.% Ni in relation to gas yield from the pyrolysis-catalytic hydrogenation of waste wood with different support materials (final pyrolysis temperature of 800 °C, catalyst temperature of 500 °C and H_2 gas hourly space velocity of 3600 ml h^{-1} g^{-1} catalyst).

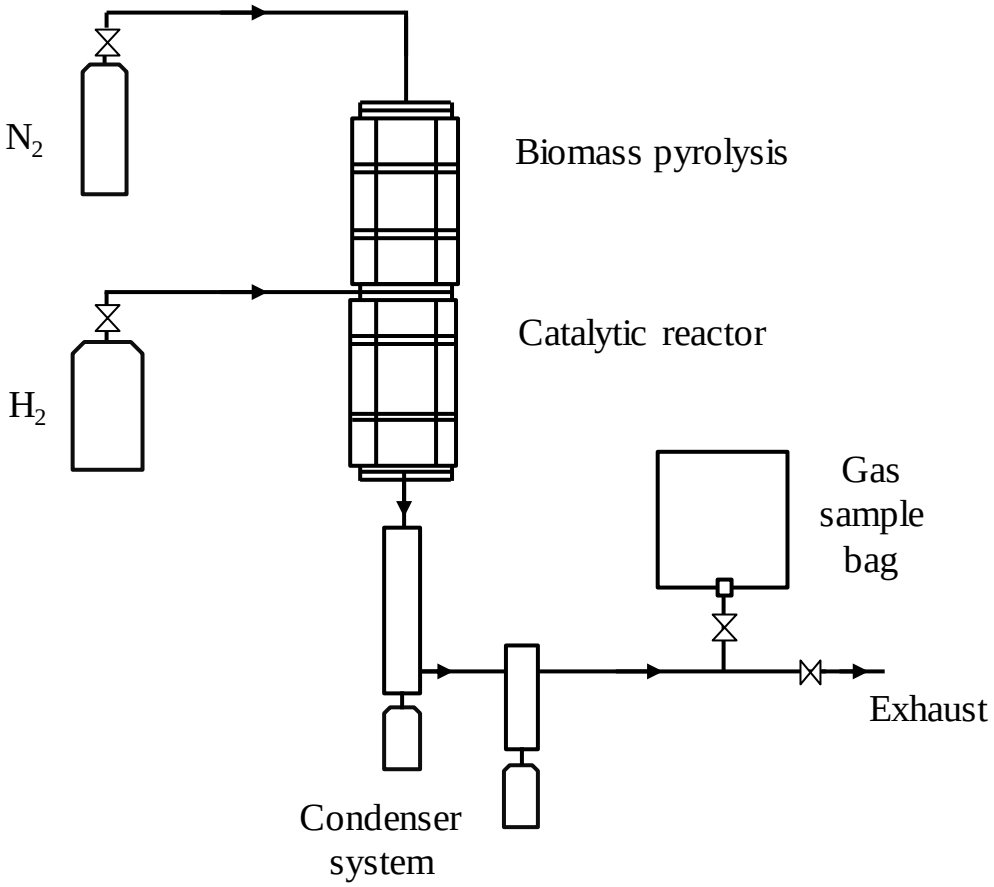

Figure 1. Schematic diagram of the two-stage pyrolysis-catalytic hydrogenation fixed bed reactor.

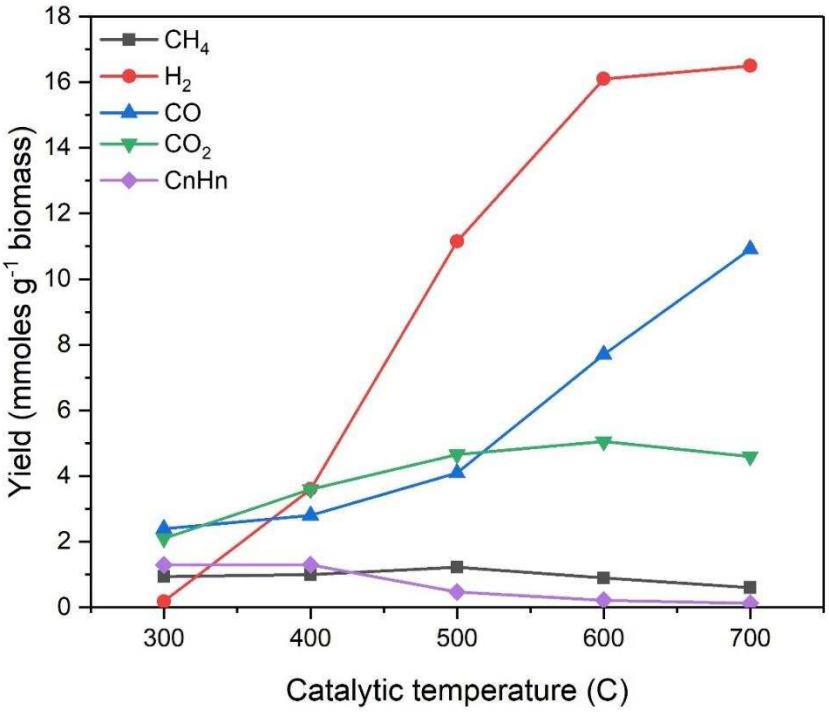

Figure 2. Influence of catalyst temperature on gas yield from the pyrolysis-catalysis of waste wood (pyrolysis temperature, 600 °C).

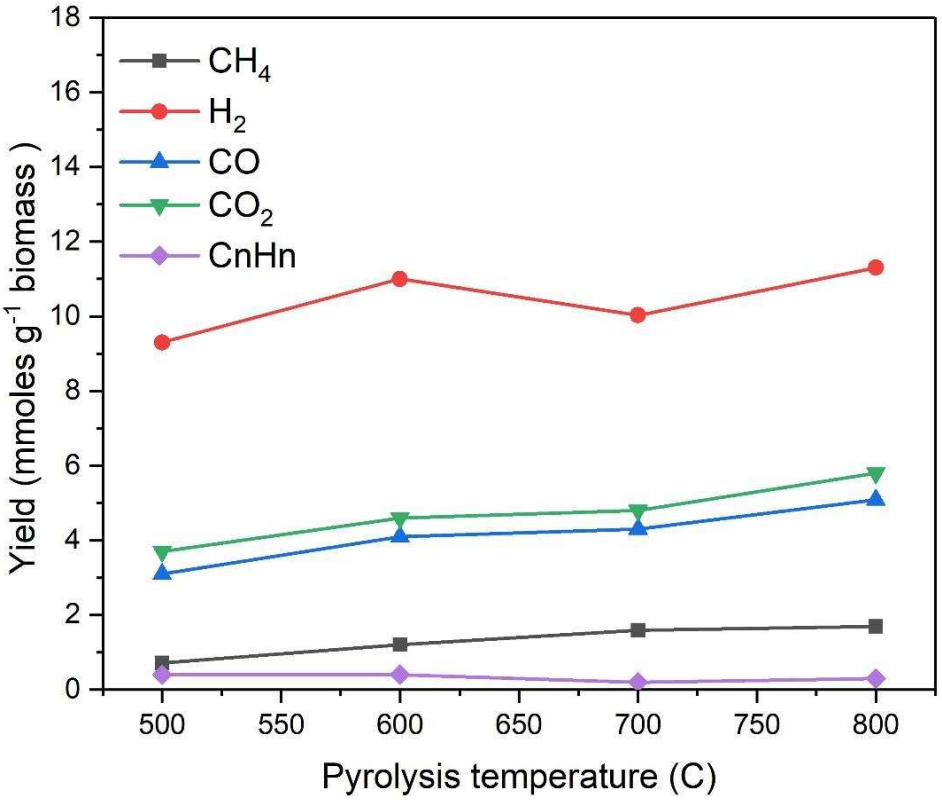

Figure 3 Influence of pyrolysis temperature on gas composition during pyrolysis-catalysis of waste wood (catalyst temperature; 500 °C).

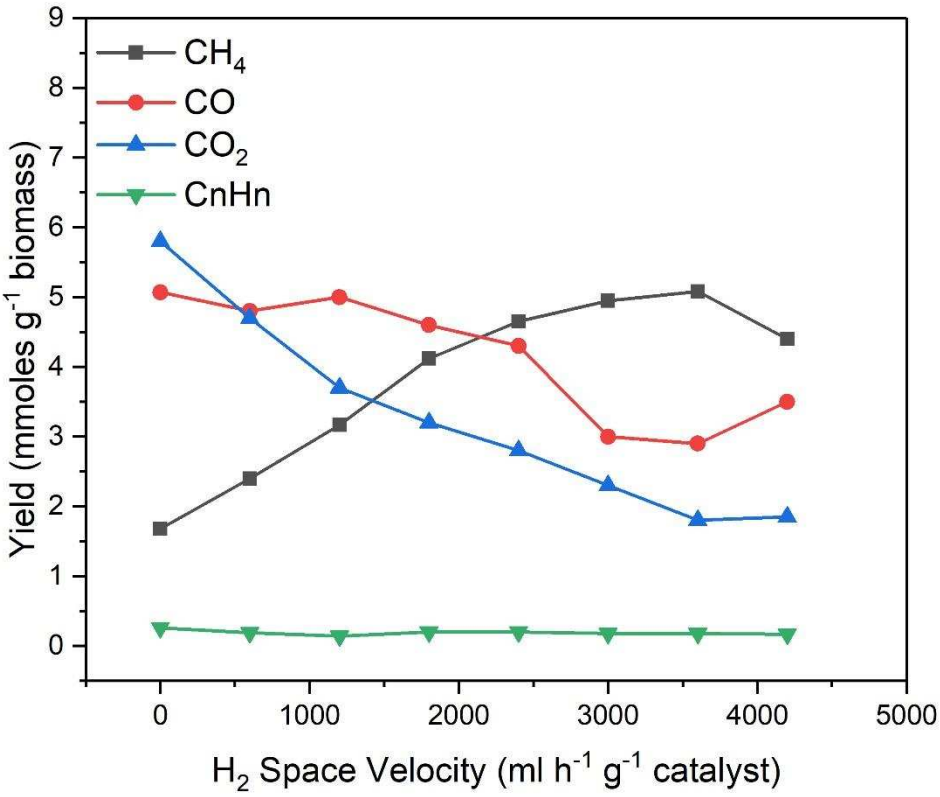

Figure 4. Influence of hydrogen gas hourly space velocity on gas composition from the pyrolysis-catalytic hydrogenation of waste wood with 10 wt.% Co/Al_2O_3 catalyst (final pyrolysis temperature of 800 °C and catalyst temperature of 500 °C).

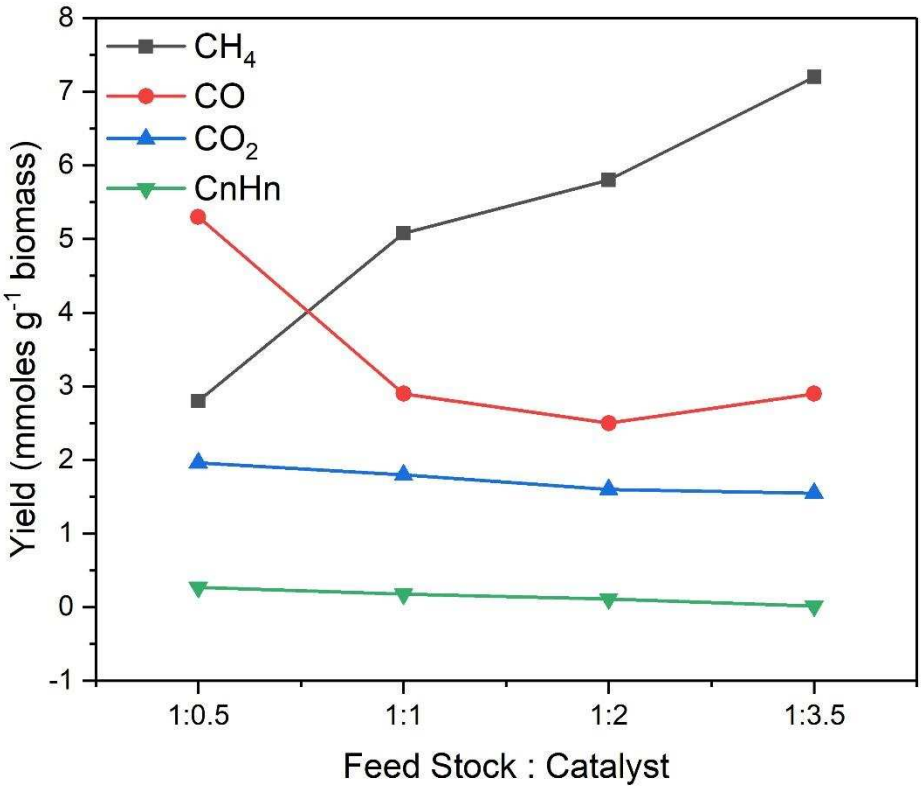

Figure 5. Influence of biomass:catalyst ratio on the gas yield from the pyrolysis-catalytic hydrogenation of waste wood with 10 wt.% Co/Al_2O_3 catalyst (final pyrolysis temperature of 800 °C, catalyst temperature of 500 °C and H_2 space velocity 3600 ml h^{-1} $g^{-1}_{catalyst}$).

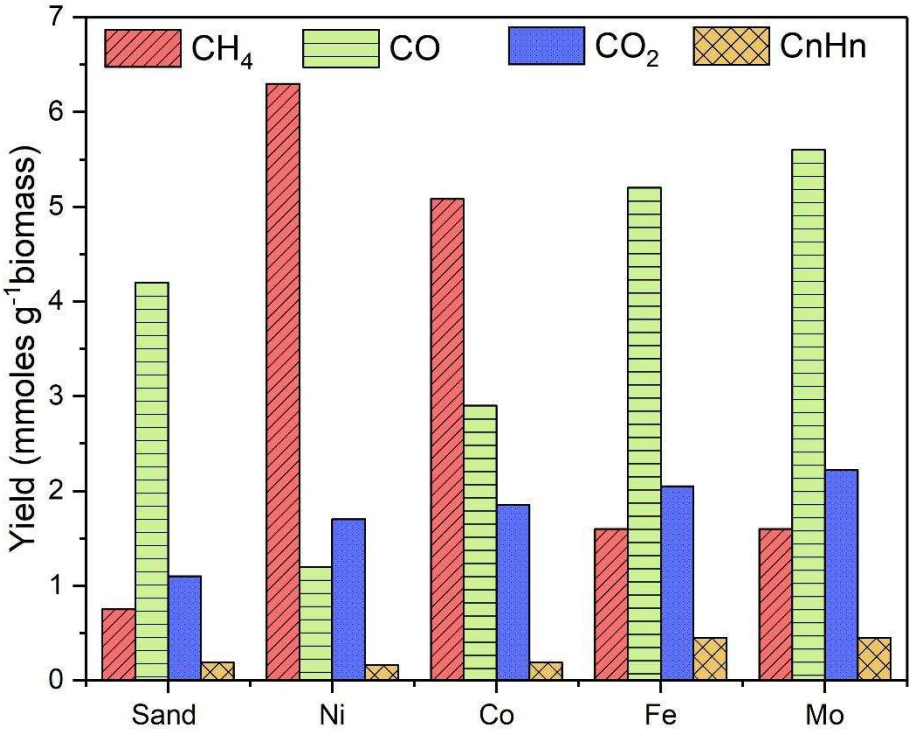

Figure 6. Influence of 10 wt.% Ni-Al_2O_3, Fe-Al_2O_3, Co-Al_2O_3 and Mo-Al_2O_3 catalysts on the gas yield from the pyrolysis-catalytic hydrogenation of waste wood (final pyrolysis temperature of 800 °C, catalyst temperature of 500 °C and H_2 gas hourly space velocity of 3600 ml h^{-1} $g^{-1}_{catayst}$).

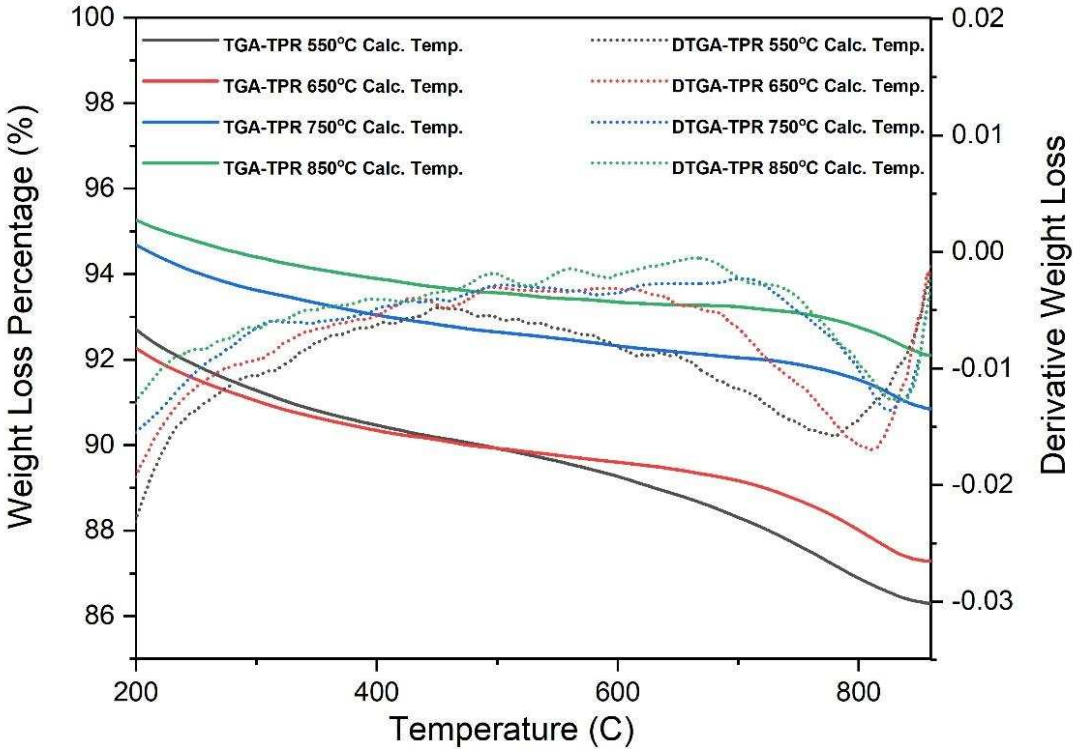

Figure 7. H_2-TPR of various 10 wt. % Ni/Al2O3 catalyst calcined at different calcination temperatures.

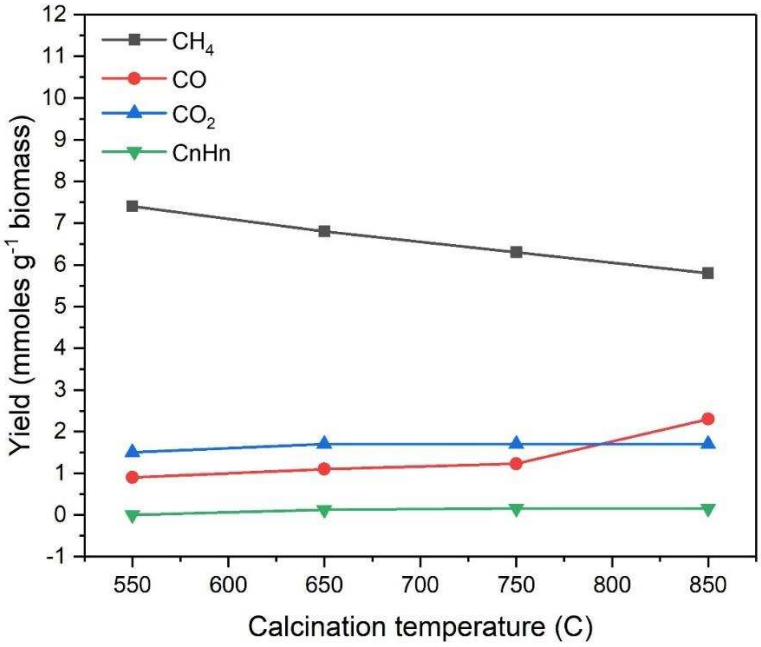

Figure 8. Influence of calcination temperature for the 10 wt.% Ni/Al_2O_3 catalyst preparation on the gas yield from the pyrolysis-catalytic hydrogenation of waste wood (final pyrolysis temperature of 800 °C, catalyst temperature of 500 °C and H_2 gas hourly space velocity of 3600 ml h^{-1} $g^{-1}_{catayst}$).

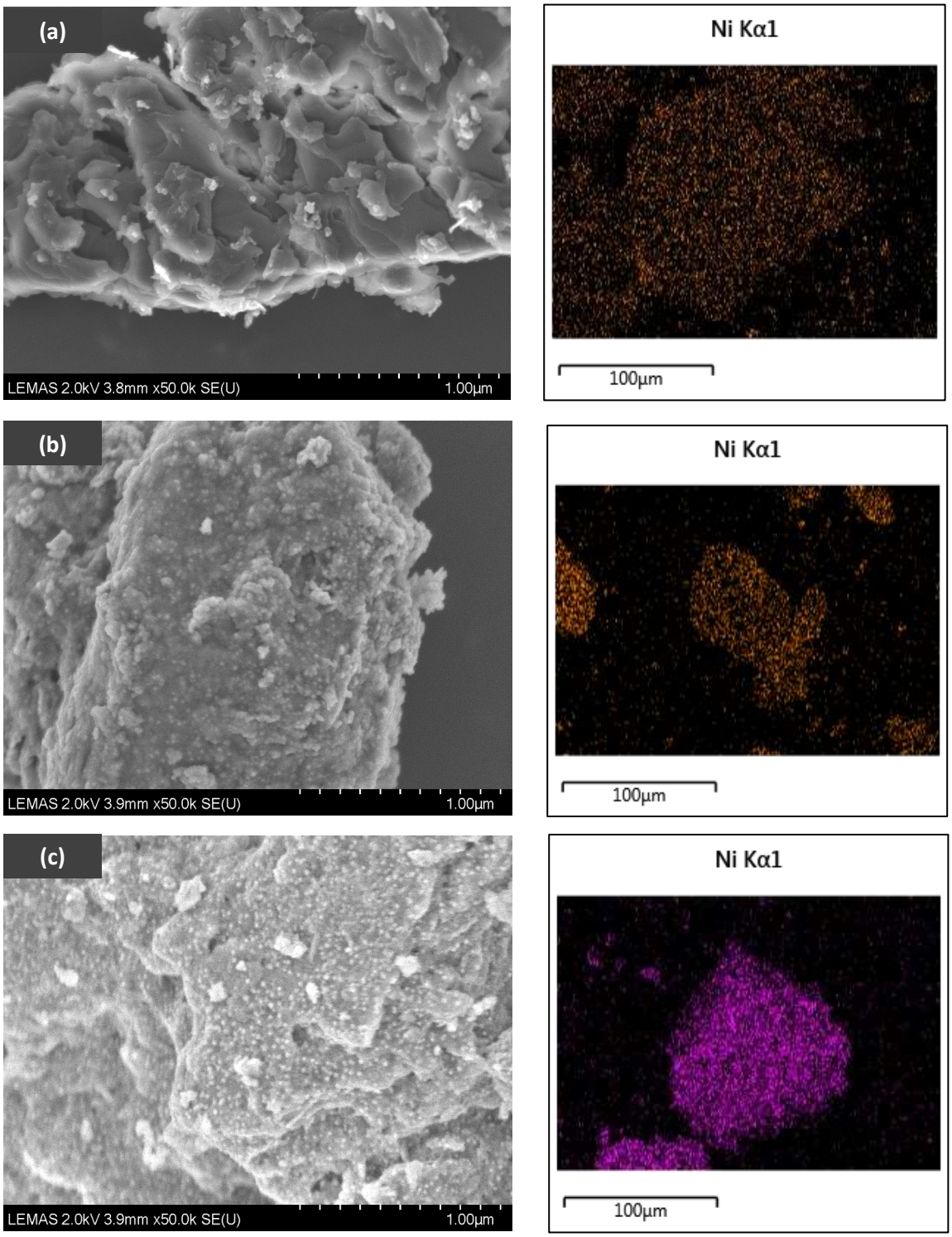

Figure 9. SEM-EDXS mapping of different nickel loadings on alumina support (a) 5 wt.%-Ni/Al_2O_3 (b) 10 wt.%/Al_2O_3Ni (c) 15 wt.%-Ni/Al_2O_3

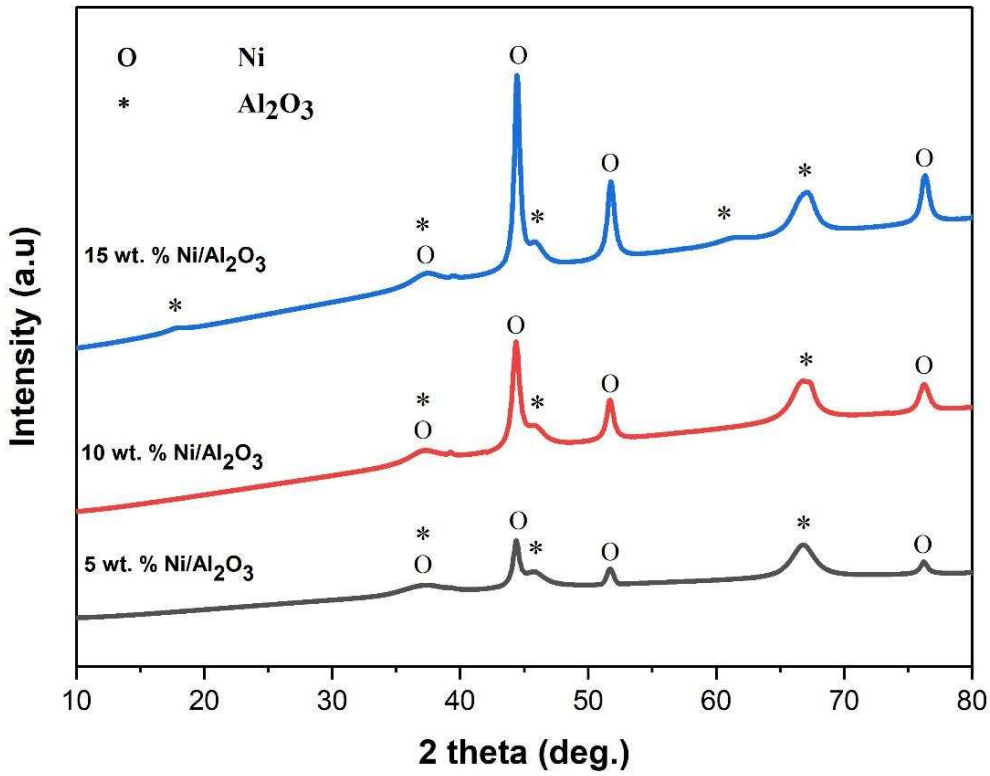

Figure 10. XRD patterns of various Ni loadings on Al_2O_3 support.

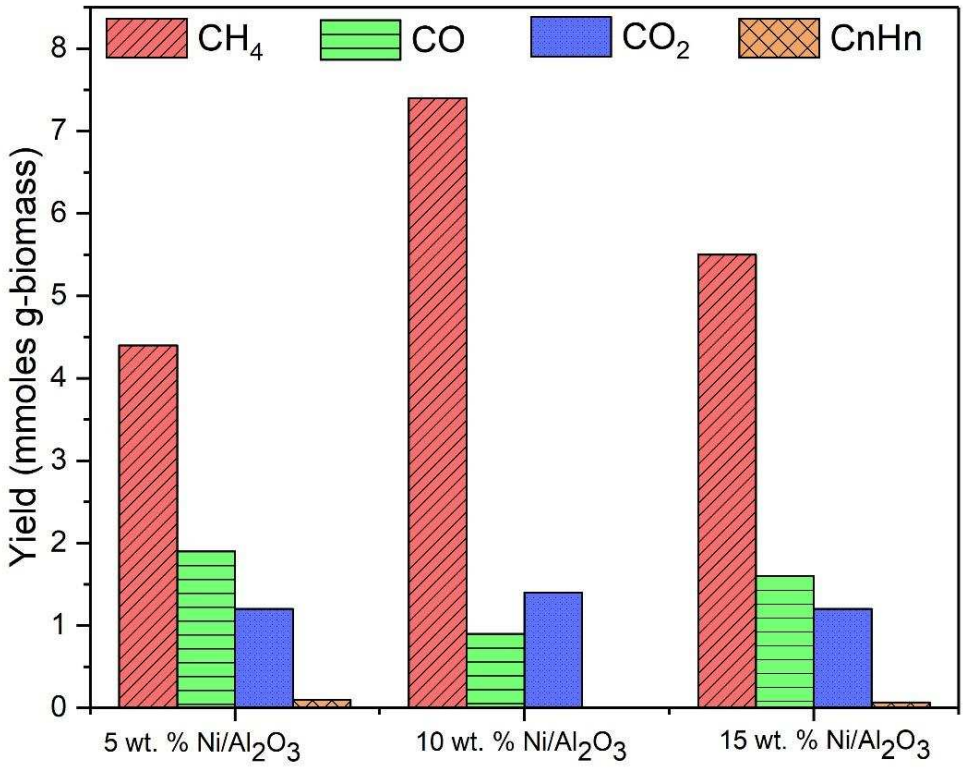

Figure 11. Influence of Ni metal loading on Ni/Al_2O_3 catalyst on the gas yield from the pyrolysis-catalytic hydrogenation of waste wood (final pyrolysis temperature of 800 °C, catalyst temperature of 500 °C and H_2 gas hourly space velocity of 3600 ml h^{-1} $g^{-1}_{catayst}$).

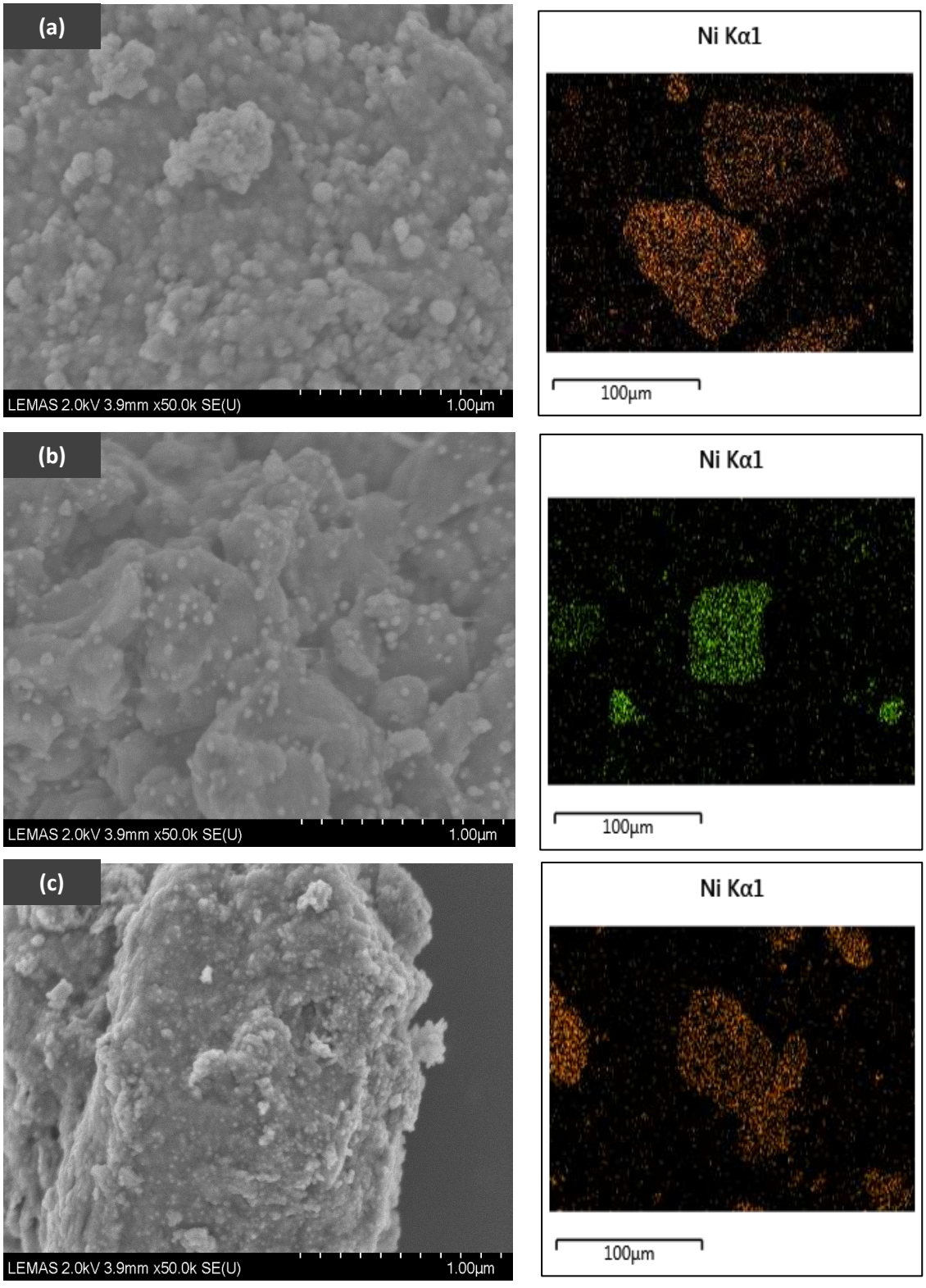

Figure 12. SEM- with EDX nickel mapping patterns of different catalyst support materials (a) 10 wt.% Ni/SiO_2 (b) 10 wt.% Ni/MCM-41 (c) 10 wt.% Ni/Al_2O_3.

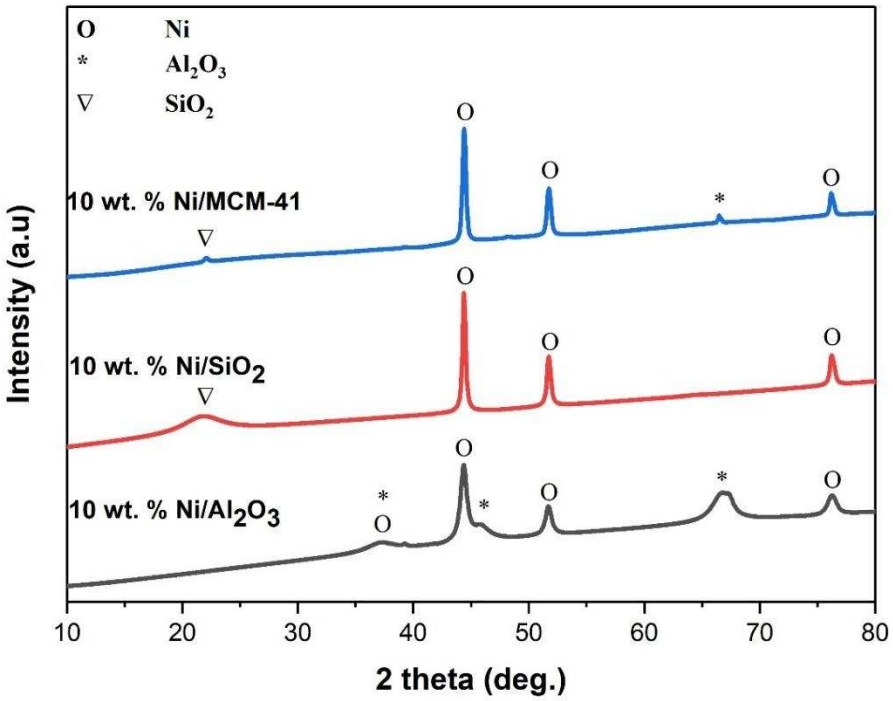

Figure 13. XRD patterns of Ni catalyst with different supports.

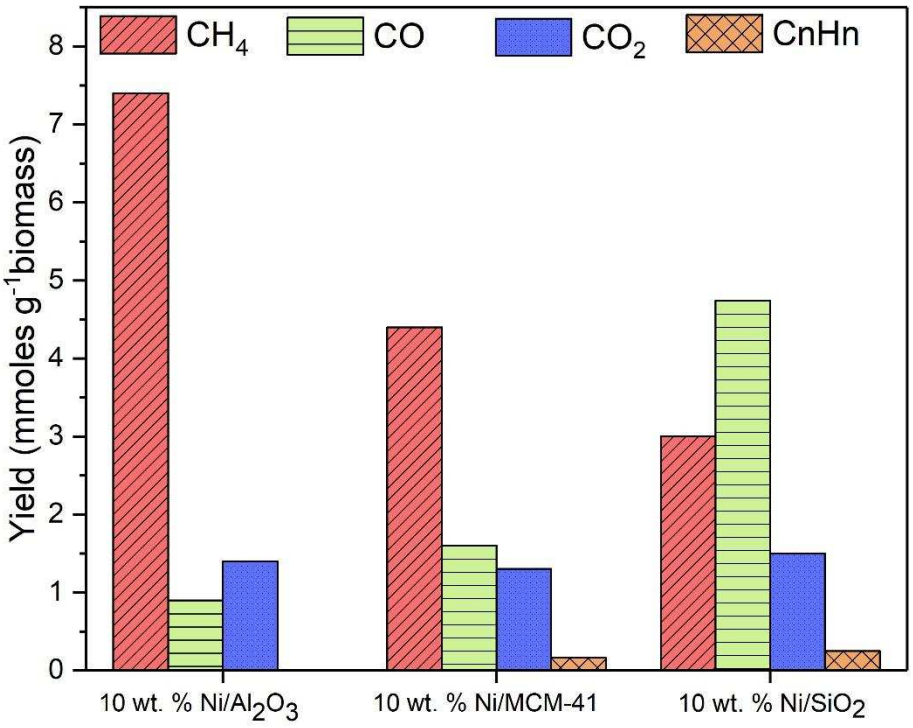

Figure 14. Influence of 10 wt.% Ni in relation to gas yield from the pyrolysis-catalytic hydrogenation of waste wood with different support materials (final pyrolysis temperature of 800 °C, catalyst temperature of 500 °C and H_2 gas hourly space velocity of 3600 ml h^{-1} g^{-1} catalyst).

Table 1. Potential reactions from the pyrolysis-catalytic hydrogenation of biomass.

Process	Reactions	Equation number
Biomass pyrolysis	$Biomass \rightarrow H_2O + H_2 + CO + CO_2 + C_xH_yO_z + C_xH_y + Char$	(1)
Bio-oil cracking	$C_xH_yO_z \rightarrow H_2O + H_2 + CO + CO_2 + CH_4 + C_nH_m$	(2)
Bio-oil auto-steam reforming	$C_xH_yO_z + H_2O \rightarrow H_2 + CO$	(3)
Hydrocarbons auto-steam reforming	$C_nH_m + H_2O \rightarrow H_2 + CO$	(4)
Bio-oil dry (CO_2) reforming	$C_xH_yO_z + CO_2 \rightarrow CO + H_2$	(5)
Hydrocarbons dry (CO_2) reforming	$C_nH_m + CO_2 \rightarrow CO + H_2$	(6)
Water gas shift reaction	$CO + H_2O \rightarrow CO_2 + H_2$	(7)
Methanation reaction (CO_2)	$CO_2 + 4H_2 \rightarrow CH_4 + 2H_2O$	(8)
Methanation reaction (CO)	$CO + 3H_2 \rightarrow CH_4 + 2H_2O$	(9)
Boudouard reaction	$2CO \rightarrow C + CO_2$	(10)
Carbon hydrogasification	$C + 2H_2 \rightarrow CH_4$	(11)

$C_xH_yO_z$ represents bio-oil and C_nH_m represents bio-oil hydrocarbons of lower molecular weight

Table 2. Influence of catalyst temperature on the product yield and gas composition from the pyrolysis-catalysis of waste wood with 10 wt.% Co/Al_2O_3 catalyst and final pyrolysis temperature of 600 °C.

	Catalyst Temperature (°C)					
	300 (sand)	**300**	**400**	**500**	**600**	**700**
Product yield (wt.%)						
Gas	30.46	34.5	40.70	49.45	61.53	66.53
Liquid	44.78	34.9	28.92	24	13.64	8.36
Solid	24.7	30.5	30.37	27.21	24.81	25.0
Gas ratios						
H_2/CO	0.85	0.73	1.28	2.71	2.07	1.50
H_2/CO_2	0.87	0.87	1.37	2.4	3.18	3.55
CH_4/CO	0.36	0.37	0.35	0.30	0.11	0.054
CH_4/CO_2	0.37	0.44	0.37	0.26	0.17	0.13
CO/CO_2	1.02	1.18	1.06	0.88	1.53	2.35
Gas composition (vol.%)						
H_2	23.6	21.1	31.8	51.5	53.6	50.3
CH_4	10.2	10.8	8.6	5.7	3.0	1.8
CO	27.7	28.8	24.7	19	25.8	33.4
CO_2	27.0	24.2	23.2	21.6	16.8	14.1
CnHn	11.4	15.0	11.8	2.2	0.8	0.4

Table 3. Influence of pyrolysis temperature on the product yield and gas composition from the pyrolysis catalysis of waste wood with 10 wt.% Co/Al_2O_3 catalyst and catalyst temperature maintained at 500 °C.

	Pyrolysis Temperature (°C)				
	500 (sand)	**500**	**600**	**700**	**800**
Product yield (wt.%)					
Gas	32.55	50.22	49.45	51.65	52
Liquid	34.4	9.95	23.32	21.48	26
Solid	33.03	39.82	27.21	26.85	22
Gas ratios					
H_2/CO	1.64	3.02	2.71	2.21	2.2
H_2/CO_2	1.42	2.47	2.4	1.97	1.96
CH_4/CO	0.31	0.23	0.30	0.37	0.33
CH_4/CO_2	0.27	0.19	0.26	0.33	0.28
CO/CO_2	0.86	0.81	0.88	0.88	0.87
Gas composition (vol.%)					
H_2	36	53	51.5	48	48
CH_4	6.9	4.2	5.7	7.6	7
CO	21.9	17.8	19	20.5	21
CO_2	25.3	21.8	21.6	23	24
CnHn	9.9	2.4	2.2	1.1	1.1

Table 4. Influence of H_2 gas hourly space velocity on the product yield and gas composition from the pyrolysis-catalytic hydrogenation of waste wood with 10 wt.% Co/Al_2O_3 catalyst (final pyrolysis temperature of 800 °C and catalyst temperature of 500 °C).

	Hydrogen Space Velocity (ml h^{-1} $g^{-1}_{catalyst}$)							
	0	**600**	**1200**	**1800**	**2400**	**3000**	**3600**	**4200**
Product yield (wt.%)								
Gas	52.0	52.0	52.0	51.6	55.2	59.0	60.0	66.8
Liquid	26.0	26.0	28.0	38.0	36.0	37.0	40.0	40.0
Solid	21.6	22.0	20.7	20.0	20.0	19.0	19.0	19.0
Gas ratios								
CH_4/CO	0.33	0.51	0.62	0.88	1.07	1.63	1.74	1.2
CH_4/CO_2	0.28	0.50	0.85	1.26	1.61	2.14	2.76	2.38
Gas composition (vol.%)								
CH_4	13.1	20.0	26.2	33.6	38.5	47.3	50.7	43.4
CO	39.5	39.4	41.0	38.0	35.9	29.0	29.1	36.8
CO_2	45.3	39.0	30.9	26.7	24	22	18.4	18.2
CnHn	2.0	1.6	1.2	1.7	1.7	1.7	1.9	1.6

Table 5. Influence of biomass:catalyst ratio on the product yield and gas composition from the pyrolysis-catalytic hydrogenation of waste wood with 10 wt.% Co/Al_2O_3 catalyst (final pyrolysis temperature of 800 °C, catalyst temperature of 500 °C and H_2 gas hourly space velocity of 3600 ml h^{-1} $g^{-1}_{catayst}$).

	Biomass:Catalyst Ratio			
	1:0.5	**1:1**	**1:2**	**1:3.5**
Product yield (wt.%)				
Gas	62.5	61.0	62.6	61.4
Liquid	38.0	40.0	42.0	38.0
Solid	19.0	19.0	19.0	19.0
Gas ratios				
CH_4/CO	0.54	1.74	2.4	2.5
CH_4/CO_2	1.46	2.76	3.57	4.62
Gas yield (vol.% H_2 free basis)				
CH_4	27.6	50.7	58.5	60.8
CO	50.9	29.1	24	25
CO_2	18.9	18.4	16.4	13.2
CnHn	2.6	1.9	1.1	0.1

Table 6. Influence of 10 wt.% Ni-Al_2O_3, Fe-Al_2O_3, Co-Al_2O_3 and Mo-Al_2O_3 catalysts on the product yield and gas composition from the pyrolysis-catalytic hydrogenation of waste wood (final pyrolysis temperature of 800 °C, catalyst temperature of 500 °C , H_2 gas hourly space velocity of 3600 ml h^{-1} $g^{-1}_{catayst}$ and Biomass:Catalyst ratio of 1:1).

	Metal Catalysts				
	Sand	**Ni/Al_2O_3**	**Co/Al_2O_3**	**Fe/Al_2O_3**	**Mo/Al_2O_3**
Product yield (wt.%)					
Gas	50.0	55.3	61.0	70.3	66.0
Liquid	32.0	30.0	40.0	22.0	18.0
Solid	19.0	19.0	19.0	19.0	19.0
Gas ratios					
CH_4/CO	0.17	5.05	1.74	0.29	0.29
CH_4/CO_2	0.66	3.6	2.76	0.78	0.72
Gas composition (vol.% H_2 free basis)					
CH_4	12	66.9	50.7	17.3	16.4
CO	66.9	13.2	29.1	55.9	56.7
CO_2	18.1	18.2	18.4	22.0	22.5
CnHn	3.0	1.7	1.9	4.8	4.4

Table 7. Physical properties of 10 % Ni/Al_2O_3 catalysts calcined at different temperature.

Calcination temperature (°C)	**Surface area (m^2 g^{-1})**	**BJH adsorption pore size (nm)**	**BJH adsorption pore volume (cm^3 g^{-1})**
550 °C	232.76	6.25	0.39
650 °C	200.44	7.56	0.39
750 °C	152.78	9.54	0.37
850 °C	136.78	10.33	0.37

Table 8. Influence of calcination temperature of catalysts on the gas yield from the pyrolysis-catalytic hydrogenation of waste wood with 10 wt.% Ni/Al_2O_3 catalyst (final pyrolysis temperature of 800 °C, catalyst temperature of 500 °C , H_2 gas hourly space velocity of 3600 ml h^{-1} $g^{-1}_{catayst}$ and Biomass:Catalyst ratio of 1:1).

	Calcination Temperature (°C)			
	550	**650**	**750**	**850**
Gas ratios				
CH_4/CO	7.52	6	5.05	2.5
CH_4/CO_2	5.2	3.94	3.6	3.34
Gas concentration (vol.% H_2 free basis)				
CH_4	75.5	69.5	66.9	57.8
CO	10	11.6	13.2	23.4
CO_2	14.5	17.6	18.2	23.4
CnHn	0	1.3	1.7	1.5

Table 9. Influence of Ni metal loading on Ni/Al_2O_3 catalyst on the gas yield from the pyrolysis-catalytic hydrogenation of waste wood (final pyrolysis temperature of 800 °C, catalyst temperature of 500 °C, H_2 gas hourly space velocity of 3600 ml h^{-1} $g^{-1}_{catayst}$ and Biomass:Catalyst ratio of 1:1).

	Metal Loading (%)		
	5%	**10%**	**15%**
Gas ratios			
CH_4/CO	2.32	7.52	3.46
CH_4/CO_2	3.7	5.2	4.64
Gas concentration (vol.% H_2 free basis)			
CH_4	58.1	75.5	66.0
CO	25	10	19.1
CO_2	15.7	14.5	14.2
CnHn	1.3	0	0.8

Table 10. Influence of 10 wt.% Ni on different support materials on the gas composition from the pyrolysis-catalytic hydrogenation of waste wood (final pyrolysis temperature of 800 °C, catalyst temperature of 500 °C, H_2 gas hourly space velocity of 3600 ml h^{-1} $g^{-1}_{catayst}$ and Biomass:Catalyst ratio of 1:1).

	Support material		
	Al_2O_3	**MCM-41**	**SiO_2**
Gas ratios			
CH_4/CO	7.52	2.68	0.62
CH_4/CO_2	5.2	3.2	1.96
Gas concentration (vol.% H_2 free basis)			
CH_4	75.5	58.4	31.4
CO	10	21.7	50
CO_2	14.5	17.8	16
CnHn	0	2.1	2.6